CTPU-15-29
KIAS-P15067
UT-HET-110

arXiv:1512.09048v2 [hep-ph] 16 Oct 2016

LHC 750 GeV Diphoton excess in a radiative seesaw model

Shinya Kanemura, [a] **Kenji Nishiwaki,** [b] **Hiroshi Okada,** [c]
Yuta Orikasa, [d] **Seong Chan Park,** [e] **Ryoutaro Watanabe** [f]

[a] *Department of Physics, University of Toyama, 3190 Gofuku, Toyama 930-8555, Japan*

[b,d,e] *School of Physics, Korea Institute for Advanced Study, Seoul 02455, Republic of Korea*

[c] *Physics Division, National Center for Theoretical Sciences, National Tsing-Hua University, Hsinchu 30013, Taiwan*

[d] *Department of Physics and Astronomy, Seoul National University, Seoul 08826, Republic of Korea*

[e] *Department of Physics and IPAP, Yonsei University, Seoul 03722, Republic of Korea*

[f] *Center for Theoretical Physics of the Universe, Institute for Basic Science (IBS), Daejeon, 34051, Republic of Korea*

18 October 2016

Abstract

We investigate a possibility for explaining the recently announced 750 GeV diphoton excess by the ATLAS and the CMS experiments at the CERN LHC in a model with multiple doubly charged particles, which was originally suggested for explaining tiny neutrino masses through a three-loop effect in a natural way. The enhanced radiatively generated effective coupling of a new singlet scalar S with diphoton with multiple charged particles in the loop enlarges the production rate of S in $pp \to S + X$ via photon fusion process and also the decay width $\Gamma(S \to \gamma\gamma)$ even without assuming a tree level production mechanism. We provide detailed analysis on the cases with or without allowing the mixing between S and the standard model Higgs doublet.

[a] E-mail: kanemu@sci.u-toyama.ac.jp
[b] E-mail: nishiken@kias.re.kr
[c] E-mail: macokada3hiroshi@gmail.com
[d] E-mail: orikasa@kias.re.kr
[e] E-mail: sc.park@yonsei.ac.kr
[f] E-mail: wryou1985@ibs.re.kr

1 Introduction

In the mid of December 2015, both of the ATLAS and CMS experiments announced the observation of a new resonance around 750 GeV as a bump in the diphoton invariant mass spectrum from the run-II data in $\sqrt{s} = 13\,\text{TeV}$ [1, 2]. Their results are based on the accumulated data of $3.2\,\text{fb}^{-1}$ (ATLAS) and $2.6\,\text{fb}^{-1}$ (CMS), and local/global significances are $3.9\sigma/2.3\sigma$ (ATLAS) [1] and $2.6\sigma/\lesssim 1.2\sigma$ (CMS) [2], respectively. The best-fit values of the invariant mass are 750 GeV by ATLAS and 760 GeV by CMS, where the ATLAS also reported the best-fit value of the total width as 45 GeV.

During/after Moriond EW in March 2016, updated results were reported with the new analysis with the different hypotheses on spin (spin-0 or spin-2) and the width to mass ratio ($\Gamma/m < 1\%$ 'narrow width' or $\Gamma/m \sim 6 - 10\%$ 'wide width') [3, 4]. Based on the $3.2\,\text{fb}^{-1}$ dataset, the ATLAS group claimed that the largest deviation from the background-only hypothesis was observed near a mass of 750 GeV, which corresponds to a local excess of 3.9σ for the spin-0 case of $\Gamma \approx 45\,\text{GeV}$ ($\Gamma/m \approx 6\%$). However, we note that the preference of the 'wide width' compared with 'narrow width' is only minor by $\sim 0.3\sigma$ significance so that we would take it with cautious attention. In our analysis below, we simply allow both cases with narrow and wide widths. The global significance is still low $\sim 2.0\sigma$.

On the other hand, based on the upgraded amount of the data of $3.3\,\text{fb}^{-1}$, the CMS group reported a modest excess of events at 760 GeV with a local significance of $2.8 - 2.9\sigma$ depending on the spin hypothesis. The 'narrow width' ($\Gamma/m = 1.4 \times 10^{-2}$) maximizes the local excess. In addition, the CMS reported the result of a combined analysis of 8 TeV and 13 TeV data, where the largest excess (3.4σ) was observed at 750 GeV for the narrow width ($\Gamma/m = 1.4 \times 10^{-4}$). The global significances are $< 1\sigma$ (1.6σ) in the 13 TeV (8 TeV + 13 TeV) analyses, respectively. No official combined (ATLAS & CMS) result has been made so far.

Just after the advent of the first announcement, various ways for explaining the 750 GeV excess have been proposed even within December 2015 in Refs. [5–125]. The first unofficial interpretation of the excess in terms of the signal strength of a scalar (or a pseudoscalar) resonance S, $pp \to S + X \to \gamma\gamma + X$, was done immediately after the first announcement in Ref. [11] based on the expected and observed exclusion limits in both of the experiments. The authors claimed,

$$\mu_{13\text{TeV}}^{\text{ATLAS}} = \sigma(pp \to S + X)_{13\text{TeV}} \times \mathcal{B}(S \to \gamma\gamma) = (10^{+4}_{-3})\,\text{fb}, \tag{1.1}$$

$$\mu_{13\text{TeV}}^{\text{CMS}} = \sigma(pp \to S + X)_{13\text{TeV}} \times \mathcal{B}(S \to \gamma\gamma) = (5.6 \pm 2.4)\,\text{fb}, \tag{1.2}$$

with a Poissonian likelihood function (for the ATLAS measurement) and the Gaussian approximation (for the CMS measurement), respectively.

On the other hand, both of the ATLAS and CMS groups reported that no significant excess over the standard model (SM) background was observed in their analyses based on the run-I data at $\sqrt{s} = 8\,\text{TeV}$ [126, 127], while a mild upward bump was found in their data around 750 GeV. In Ref. [11], the signal strengths at $\sqrt{s} = 8\,\text{TeV}$ were extracted by use of the corresponding expected and observed exclusion limits given by the experiments, in the Gaussian approximation, for a narrow-width scalar resonance as

$$\mu_{8\text{TeV}}^{\text{ATLAS}} = \sigma(pp \to S + X)_{8\text{TeV}} \times \mathcal{B}(S \to \gamma\gamma) = (0.46 \pm 0.85)\,\text{fb}, \tag{1.3}$$

$$\mu_{8\text{TeV}}^{\text{CMS}} = \sigma(pp \to S + X)_{8\text{TeV}} \times \mathcal{B}(S \to \gamma\gamma) = (0.63 \pm 0.35)\,\text{fb}. \tag{1.4}$$

It is mentioned that when we upgrade the collider energy from 8 TeV to 13 TeV, a factor 4.7 enhancement is expected [11, 128], when the resonant particle is produced via gluon fusion, and

then the data at $\sqrt{s} = 8\,\text{TeV}$ and $13\,\text{TeV}$ are compatible at around 2σ confidence level (C.L.). Indeed, in the second announcement [3], the ATLAS group discussed this point based on the reanalyzed 8 TeV data corresponding to an integrated luminosity of $20\,\text{fb}^{-1}$ with the latest photon energy calibration in the run-I, which is close to the calibration used for the 13 TeV data. When $m = 750\,\text{GeV}$ and $\Gamma/m = 6\%$, the difference between the 8 TeV and 13 TeV results corresponds to statistical significances of 1.2σ (2.1σ) if gluon-gluon (quark-antiquark) productions are assumed. These observations would give us a stimulating hint for surveying the structure of physics beyond the SM above the electroweak scale even though the accumulated amount of the data would not be enough for detailed discussions and the errors are large at the present stage.

A key point to understand the resonance is the fact that no bump around 750 GeV has been found in the other final states in both of the 8 TeV and 13 TeV data. If $\mathcal{B}(S \to \gamma\gamma)$ is the same as the 750 GeV Higgs one, $\mathcal{B}(h \to \gamma\gamma)|_{750\,\text{GeV SM}} = 1.79 \times 10^{-7}$ [129], we can immediately recognize that such a possibility is inconsistent with the observed results, e.g., in ZZ final state, at $\sqrt{s} = 8\,\text{TeV}$, where the significant experimental 95% C.L. upper bound on the ZZ channel is 12 fb by ATLAS [130] and the branching ratio $\mathcal{B}(h \to ZZ)|_{750\,\text{GeV SM}} = 0.290$ [129]. In general, the process $S \to \gamma\gamma$ should be loop induced since S has zero electromagnetic charge and then the value of $\mathcal{B}(S \to \gamma\gamma)$ tends to be suppressed because tree level decay branches generate primary components of the total width of S. Then, a reasonable setup for explaining the resonance consistently is that all of the decay channels of S are one loop induced, where S would be a gauge singlet under $SU(3)_C$ and $SU(2)_L$ since a non-singlet gauge assignment leads to tree level gauge interactions, which are not desired in our case.

An example of this direction is that S is a singlet scalar and it couples to vector-like quarks, which contribute to both of $pp \to S + X$ and $S \to \gamma\gamma$ via gluon fusion and photon fusion, respectively. The possibility of diphoton production solely due to photon fusion is also an open possibility as discussed in Refs. [34, 40] in the context of the 750 GeV excess. Basic idea is simple: when a model contains multiple $SU(2)_L$ singlet particles with large $U(1)_Y$ hypercharges, the magnitude of the photon fusions in the production and decay sequences is largely enhanced.

In this paper, we focus on the radiative seesaw models [131–135], especially where neutrino masses are generated at the three loop level [136–153]. In such type of scenarios, multiple charged scalars are introduced for realizing three-loop origin of the neutrino mass, (distinctively from the models with one or two loops). We show that when these charged scalars couple to the singlet S strongly enough, we can achieve a reasonable amount of the production cross section in $pp \to S + X \to \gamma\gamma + X$ through photon fusion. Concretely, we start from the three loop model [150], and extend the model with additional charged scalars to explain the data.[1]

This paper is organized as follows. In Sec. 2, we introduce our model based on the model for three-loop induced neutrino masses. In Sec. 3, we show detail of analysis and numerical results. In Sec. 4, we are devoted to summary and discussions.

2 Model

Multiple (doubly) charged particles would induce a large radiative coupling with a singlet scalar S with $\gamma\gamma$ via one-loop diagrams. We may find the source from multi-Higgs models or extra dimensions [160–177] but here we focus on a model for radiative neutrino masses recently suggested by some of the authors [150] as a benchmark model, which can be extended with a singlet scalar S for the 750 GeV resonance.

[1] Recently, several other works have emerged in this direction [154–159].

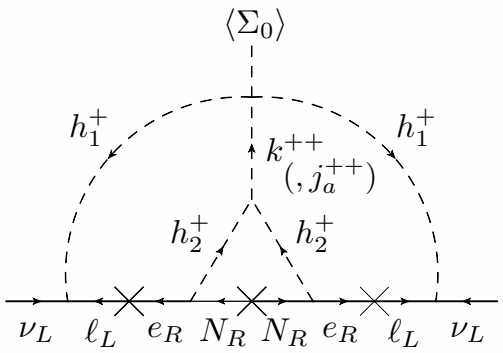

Figure 1: A schematic description for the radiative generation of neutrino masses.

2.1 Review: A model for three-loop induced neutrino mass

Our strategy is based on the three loop induced radiative neutrino model with a $U(1)$ global symmetry [150], where we introduce three Majorana fermions $N_{R_{1,2,3}}$ and new bosons; one gauge-singlet neutral boson Σ_0, two singly charged singlet scalars $(h_1^\pm, h_2^\pm)$, and one gauge-singlet doubly charged boson $k^{\pm\pm}$ to the SM. The particle contents and their charges are shown in Table 1.

	Lepton Fields			Scalar Fields					New Scalar Fields	
Characters	L_{L_i}	e_{R_i}	N_{R_i}	Φ	Σ_0	h_1^+	h_2^+	k^{++}	j_a^{++}	S
$SU(3)_C$	**1**	**1**	**1**	**1**	**1**	**1**	**1**	**1**	**1**	**1**
$SU(2)_L$	**2**	**1**	**1**	**2**	**1**	**1**	**1**	**1**	**1**	**1**
$U(1)_Y$	$-1/2$	-1	0	$1/2$	0	1	1	2	2	0
$U(1)$	0	0	$-x$	0	$2x$	0	x	$2x$	$2x$	0

Table 1: Contents of lepton and scalar fields and their charge assignment under $SU(3)_C \times SU(2)_L \times U(1)_Y \times U(1)$, where $U(1)$ is an additional global symmetry and $x \neq 0$. The subscripts found in the lepton fields $i\,(= 1, 2, 3)$ indicate generations of the fields. The bold letters emphasize that these numbers correspond to representations of the Lie groups of the NonAbelian gauge interactions. The scalar particles shown in the right category (New Scalar Fields) are added to the original model proposed in Ref. [150] to explain the 750 GeV excess.

We assume that only the SM-like Higgs Φ and the additional neutral scalar Σ_0 have VEVs, which are symbolized as $\langle\Phi\rangle \equiv v/\sqrt{2}$ and $\langle\Sigma_0\rangle \equiv v'/\sqrt{2}$, respectively. $x\,(\neq 0)$ is an arbitrary number of the charge of the hidden $U(1)$ symmetry, and under the assignments, neutrino mass matrix is generated at the three loop level, where a schematic picture is shown in Fig. 1. A remnant Z_2 symmetry remains after the hidden $U(1)$ symmetry breaking and the particles $N_{R_{1,2,3}}$ and $h_2^\pm$ have negative parities. Then, when a Majorana neutrino is the lightest among them, it becomes a dark matter (DM) candidate and the stability is accidentally ensured.

In the original model, the Lagrangian of Yukawa sector $\mathcal{L}_Y$ and scalar potential $\mathcal{V}$, allowed under the gauge and global symmetries, are given as

$$-\mathcal{L}_Y = (y_\ell)_{ij}\bar{L}_{L_i}\Phi e_{R_j} + \frac{1}{2}(y_L)_{ij}\bar{L}^c_{L_i}L_{L_j}h_1^+ + (y_R)_{ij}\bar{N}_{R_i}e^c_{R_j}h_2^- + \frac{1}{2}(y_N)_{ij}\Sigma_0\bar{N}^c_{R_i}N_{R_j} + \text{h.c.}, \quad (2.1)$$

$$\mathcal{V} = m_\Phi^2|\Phi|^2 + m_\Sigma^2|\Sigma_0|^2 + m_{h_1}^2|h_1^+|^2 + m_{h_2}^2|h_2^+|^2 + m_k^2|k^{++}|^2$$

$$+\left[\lambda_{11}\Sigma_0^* h_1^- h_1^- k^{++} + \mu_{22} h_2^+ h_2^+ k^{--} + \text{h.c.}\right] + \lambda_\Phi |\Phi|^4 + \lambda_{\Phi\Sigma}|\Phi|^2|\Sigma_0|^2 + \lambda_{\Phi h_1}|\Phi|^2|h_1^+|^2$$
$$+ \lambda_{\Phi h_2}|\Phi|^2|h_2^+|^2 + \lambda_{\Phi k}|\Phi|^2|k^{++}|^2 + \lambda_\Sigma|\Sigma_0|^4 + \lambda_{\Sigma h_1}|\Sigma_0|^2|h_1^+|^2 + \lambda_{\Sigma h_2}|\Sigma_0|^2|h_2^+|^2$$
$$+ \lambda_{\Sigma k}|\Sigma_0|^2|k^{++}|^2 + \lambda_{h_1}|h_1^+|^4 + \lambda_{h_1 h_2}|h_1^+|^2|h_2^+|^2 + \lambda_{h_1 k}|h_1^+|^2|k^{++}|^2$$
$$+ \lambda_{h_2}|h_2^+|^4 + \lambda_{h_2 k}|h_2|^2|k^{++}|^2 + \lambda_k|k^{++}|^4, \tag{2.2}$$

where the indices i, j indicate matter generations and the superscript "c" means charge conjugation (with the $SU(2)_L$ rotation by $i\sigma_2$ for $SU(2)_L$ doublets). We assume that y_N is diagonal, where the right-handed neutrino masses are calculated as $M_{N_i} = \frac{v'}{\sqrt{2}}(y_N)_{ii}$ with the assumed ordering $M_{N_1}(= \text{DM mass}) < M_{N_2} < M_{N_3}$. The neutral scalar fields are shown in the Unitary gauge as

$$\Phi = \begin{bmatrix} 0 \\ \frac{v+\phi}{\sqrt{2}} \end{bmatrix}, \quad \Sigma_0 = \frac{v'+\sigma}{\sqrt{2}} e^{iG/v'}, \tag{2.3}$$

with $v \simeq 246\,\text{GeV}$ and an associated Nambu-Goldstone (NG) boson G via the global $U(1)$ breaking due to the occurrence of nonzero v'. Requiring the tadpole conditions, $\partial\mathcal{V}/\partial\phi|_{\phi=v} = \partial\mathcal{V}/\partial\sigma|_{\sigma=v'} = 0$, the resultant mass matrix squared of the CP even components (ϕ, σ) is given by

$$m^2(\phi,\sigma) = \begin{bmatrix} 2\lambda_\Phi v^2 & \lambda_{\Phi\Sigma} v v' \\ \lambda_{\Phi\Sigma} v v' & 2\lambda_\Sigma v'^2 \end{bmatrix} = \begin{bmatrix} \cos\alpha & \sin\alpha \\ -\sin\alpha & \cos\alpha \end{bmatrix} \begin{bmatrix} m_h^2 & 0 \\ 0 & m_H^2 \end{bmatrix} \begin{bmatrix} \cos\alpha & -\sin\alpha \\ \sin\alpha & \cos\alpha \end{bmatrix}, \tag{2.4}$$

where h is the SM-like Higgs ($m_h = 125\,\text{GeV}$) and H is an additional CP even Higgs mass eigenstate. The mixing angle α is determined as

$$\sin 2\alpha = \frac{2\lambda_{\Phi\Sigma} v v'}{m_H^2 - m_h^2}. \tag{2.5}$$

The neutral bosons ϕ and σ are represented in terms of the mass eigenstates h and H as

$$\phi = h\cos\alpha + H\sin\alpha, \quad \sigma = -h\sin\alpha + H\cos\alpha. \tag{2.6}$$

The two CP even scalars h and H could work as DM-portal scalars and participate in the DM pair annihilation. The mass eigenvalues for the singly charged bosons $h_1^\pm$, $h_2^\pm$ and the doubly charged boson $k^{\pm\pm}$ are given as

$$m_{h_1^\pm}^2 = m_{h_1}^2 + \frac{1}{2}(\lambda_{\Phi h_1} v^2 + \lambda_{\Sigma h_1} v'^2), \quad m_{h_2^\pm}^2 = m_{h_2}^2 + \frac{1}{2}(\lambda_{\Phi h_2} v^2 + \lambda_{\Sigma h_2} v'^2),$$
$$m_{k^{\pm\pm}}^2 = m_k^2 + \frac{1}{2}(\lambda_{\Phi k} v^2 + \lambda_{\Sigma k} v'^2). \tag{2.7}$$

This model can explain the smallness of the observed neutrino masses and the presence of DM without severe parameter tuning. A summary of the features in the model is given in Appendix A.

Here we introduce a real singlet scalar S in the model and assume that it couples with the doubly charged scalar(s). Due to the contributions of the charged particles in the loop, a large branching ratio $\mathcal{B}(S \to \gamma\gamma)$ is achievable without assuming tree level interactions [34, 40]. When $\mathcal{B}(S \to \gamma\gamma)$ is sizable, the production cross section of the resonance particle, $\sigma(pp \to S + X)$, becomes large through photon fusion processes thus we do not have to rely on gluon fusion processes, which often requests additional colored particles that brings in dangerous hadronic activities. Thus we may explain the 750 GeV excess as pointed out in [34, 40].

2.2 Extension with a scalar S for the 750 GeV resonance

In the following part, we consider an extension of the original model with the new interactions as

$$\Delta\mathcal{V} = \hat{\mu}_{Sk} S|k^{++}|^2 + \hat{\lambda}_{Sk} S^2|k^{++}|^2 + \mathcal{V}(S) + \sum_{a=1}^{N_j} \left\{ \hat{m}^2_{j_a^{\pm\pm}} |j_a^{++}|^2 + \hat{\mu}_{Sj_a} S|j_a^{++}|^2 + \hat{\lambda}_{Sj_a} S^2 |j_a^{++}|^2 + \left[\lambda_{11}^{(a)} \Sigma_0^* h_1^- h_1^- j_a^{++} + \mu_{22}^{(a)} h_2^+ h_2^+ j_a^{--} + \text{h.c.} \right] \right\}, \tag{2.8}$$

where S is a real scalar and $j_a^{\pm\pm}$ $(a = 1, 2, \cdots, N_j)$ are additional $SU(2)_L$ singlet doubly charged scalars with hyper charge $+2$ and a global $U(1)$ charge $+2x$. $\mathcal{V}(S)$ represents the potential of the singlet scalar S. Here, we assume that S has a VEV, and S should be replaced as $S \to \langle S \rangle + S$. After the replacement, we pick up the relevant terms for our analysis and summarize,

$$\Delta\mathcal{V}_{\text{eff}} = \mu_{Sk} S|k^{++}|^2 + \frac{1}{2} m_S^2 S^2 + \sum_{a=1}^{N_j} \left\{ m^2_{j_a^{\pm\pm}} |j_a^{++}|^2 + \mu_{Sj_a} S|j_a^{++}|^2 + \left[\lambda_{11}^{(a)} \Sigma_0^* h_1^- h_1^- j_a^{++} + \mu_{22}^{(a)} h_2^+ h_2^+ j_a^{--} + \text{h.c.} \right] \right\}, \tag{2.9}$$

with

$$m^2_{j_a^{\pm\pm}} \equiv \hat{m}^2_{j_a^{\pm\pm}} + \hat{\mu}_{Sj_a} \langle S \rangle + \hat{\lambda}_{Sj_a} \langle S \rangle^2, \quad \mu_{Sk} \equiv \hat{\mu}_{Sk} + 2\hat{\lambda}_{Sk} \langle S \rangle, \quad \mu_{Sj_a} \equiv \hat{\mu}_{Sj_a} + 2\hat{\lambda}_{Sj_a} \langle S \rangle. \tag{2.10}$$

The squared physical masses of S and $j_a^{\pm\pm}$ are m_S^2 and $m^2_{j_a^{\pm\pm}}$, respectively and we set m_S as 750 GeV for our explanation of the 750 GeV excess.[2] $j_a^{\pm\pm}$ has the same charges as $k^{\pm\pm}$ and then can contribute to the three-loop induced neutrino masses shown in Fig. 1.[3] The trilinear terms in the square brackets are required for evading the stability of $j_a^{\pm\pm}$. We also ignore the possible terms as $|j_a^{++}|^2|\Phi|^2$, $|j_a^{++}|^2|\Sigma_0|^2$ and $S|\Phi|^2$, $S|\Sigma_0|^2$ in Eq. (2.8) in our analysis below. This is justified as a large VEV of S generates large effective trilinear couplings μ_{Sk} and μ_{Sj_a} through the original terms $S^2|k^{++}|$ and $S^2|j_a^{++}|$, respectively, even when the dimensionless coefficients $\hat{\lambda}_{Sk}$ and $\hat{\lambda}_{Sj_a}$ are not large.

3 Analysis

3.1 Formulation of $p(\gamma)p(\gamma) \to S + X \to \gamma\gamma + X$

Additional interactions in Eq. (2.9) provide possible decay channels of S to $\gamma\gamma$, $Z\gamma$, ZZ and $k^{++}k^{--}$ or $j_a^{++}j_a^{--}$ up to the one-loop level. We assume that $m_{k^{\pm\pm}}$ and $m_{j_a^{\pm\pm}}$ are greater than $m_S/2\,(= 375\,\text{GeV})$, where the last two decay channels at the tree level are closed kinematically. Here, we show the case when S is a mass eigenstate and there is no mixing through mass terms with other scalars. In the present case that no tree-level decay branch is open and only $SU(2)_L$ singlet charged scalars describe the loop-induced partial widths, the relative strengths among $\Gamma_{S\to\gamma\gamma}$,

[2] In a later stage of Sec. 3.2.2, we have discussions on the situation when S and Φ are mixed.

[3] In general, mixing between $k^{\pm\pm}$ and $j_a^{\pm\pm}$ could be allowed but the induced value via renormalization group running at the scale of our interest is expected to be small with heavy masses of $h_1^\pm$ and $h_2^\pm$, thus is neglected.

$\Gamma_{S\to Z\gamma}$, $\Gamma_{S\to ZZ}$ and $\Gamma_{S\to W^+W^-}$ are governed by quantum numbers at the one-loop level[4] as

$$\Gamma_{S\to\gamma\gamma} : \Gamma_{S\to Z\gamma} : \Gamma_{S\to ZZ} : \Gamma_{S\to W^+W^-} \approx 1 : 2\left(\frac{s_W^2}{c_W^2}\right) : \left(\frac{s_W^4}{c_W^4}\right) : 0. \tag{3.1}$$

In the following, we calculate $\Gamma_{S\to ZZ}$ in a simplified way of

$$\Gamma_{S\to ZZ} \approx s_W^2/(2c_W^2)\Gamma_{S\to Z\gamma} \simeq 0.15\,\Gamma_{S\to Z\gamma}. \tag{3.2}$$

Here, we represent a major part of partial decay widths of S with our notation for loop functions with the help of Refs. [179–183]. In the following part, for simplicity, we set all the masses of the doubly charged scalars $m_{j_a^{\pm\pm}}$ as the same as $m_{k^{\pm\pm}}$, while we ignore the contributions from the two singly charged scalars $h_{1,2}^{\pm}$ since they should be heavy as at least around 3 TeV and decoupled as mentioned in Appendix A. The concrete form of $\Gamma_{S\to\gamma\gamma}$ and $\Gamma_{S\to Z\gamma}$ are given as

$$\Gamma_{S\to\gamma\gamma} = \frac{\alpha_{\rm EM}^2 m_S^3}{256\pi^3 v^2}\left|\frac{1}{2}\frac{v\mu}{m_{k^{\pm\pm}}^2}Q_k^2 A_0^{\gamma\gamma}(\tau_k)\right|^2, \tag{3.3}$$

$$\Gamma_{S\to Z\gamma} = \frac{\alpha_{\rm EM}^2 m_S^3}{512\pi^3}\left(1-\frac{m_Z^2}{m_S^2}\right)^3\left|-\frac{\mu}{m_{k^{\pm\pm}}^2}\left(2Q_k g_{Zkk}\right)A_0^{Z\gamma}(\tau_k,\lambda_k)\right|^2, \tag{3.4}$$

with

$$\mu = \sum_a \mu_a \equiv \left[\mu_{Sk} + \sum_{a=1}^{N_j}\mu_{Sj_a}\right], \quad g_{Zkk} = -Q_k\left(\frac{s_W}{c_W}\right), \quad \tau_k = \frac{4m_{k^{\pm\pm}}^2}{m_S^2}, \quad \lambda_k = \frac{4m_{k^{\pm\pm}}^2}{m_Z^2}. \tag{3.5}$$

$Q_k\,(=2)$ is the electric charge of the doubly charged scalars in unit of the positron's one. c_W and s_W are the cosine and the sine of the Weinberg angle θ_W, respectively. $\alpha_{\rm EM}$ is the electromagnetic fine structure constant. In the following calculation, we use $s_W^2 = 0.23120$ and $\alpha_{\rm EM} = 1/127.916$. The loop factors take the following forms,

$$\begin{aligned} A_0^{\gamma\gamma}(x) &= -x^2\left[x^{-1} - f(x^{-1})\right], \\ A_0^{Z\gamma}(x,y) &= \frac{xy}{2(x-y)} + \frac{x^2y^2}{2(x-y)^2}\left[f(x^{-1}) - f(y^{-1})\right] + \frac{x^2y}{(x-y)^2}\left[g(x^{-1}) - g(y^{-1})\right], \end{aligned} \tag{3.6}$$

The two functions $f(z)$ and $g(z)$ ($z \equiv x^{-1}$ or y^{-1}) are formulated as

$$f(z) = \arcsin^2\sqrt{z} \quad \text{for } z \le 1, \tag{3.7}$$

$$g(z) = \sqrt{z^{-1}-1}\arcsin\sqrt{z} \quad \text{for } z \le 1, \tag{3.8}$$

where the situation $m_S \le 2m_{k^{\pm\pm}}$, $m_Z \le 2m_{k^{\pm\pm}}$ corresponds to $z \le 1$. For simplicity, we assume the relation

$$\mu_{Sk} = \mu_{Sj_a}, \tag{3.9}$$

for all a.

[4]The branching fractions are easily understood in an effective theory with the standard model gauge symmetries. See e.g. [178] with $s_2 = 0$ in the paper.

For the production of S corresponding to the 750 GeV resonance, we consider the photon fusion process, as firstly discussed in the context of the 750 GeV excess in Refs. [34, 40]. We take the photon parton distribution function (PDF) from Ref. [184], which adopted the methods in Ref. [185].[5] The inclusive production cross section of a scalar (or pseudoscalar) resonance R is generally formulated as

$$\frac{d\sigma^{\rm inc}(p(\gamma)p(\gamma)\to R+X)}{dM_R^2\,dy_R} = \frac{d\mathcal{L}^{\rm inc}}{dM_R^2\,dy_R}\hat{\sigma}(\gamma\gamma\to R), \tag{3.10}$$

where M_R and y_R are the mass and the rapidity of the resonance R, and $\hat{\sigma}(\gamma\gamma\to R)$ shows the parton-level cross section for the process $\gamma\gamma\to R$. The inclusive luminosity function can be conveniently written in terms of the photon PDF as

$$\frac{d\mathcal{L}^{\rm inc}_{\gamma\gamma}}{dM_R^2\,dy_R} = \frac{1}{s}\gamma(x_1,\mu)\,\gamma(x_2,\mu), \tag{3.11}$$

where $x_{1,2} = \frac{M_R}{\sqrt{s}}e^{\pm y_R}$ represent the momentum fractions of the photons inside the protons and $\sqrt{s}$ means the total energy. The value of $\gamma(x,\mu)$ can be evaluated by taking the Dokshitzer-Gribov-Lipatov-Altarelli-Parisi (DGLAP) evolution from the starting scale $\mu_0\,(=1\,{\rm GeV})$ to μ after an estimation of coherent and incoherent components of the initial form of $\gamma(x,\mu=\mu_0)$ at $\mu=\mu_0$ (See [184] for details.).

By adopting the narrow width approximation, which is fine in our case, the parton-level cross section of the particle S of mass m_S and rapidity y_S is given as

$$\begin{aligned}\hat{\sigma}(\gamma\gamma\to S) &= \frac{8\pi^2\Gamma(S\to\gamma\gamma)}{m_S}\delta(M_R^2-m_S^2)\\ &= \frac{8\pi^2\Gamma_{\rm tot}(S)}{m_S}\mathcal{B}(S\to\gamma\gamma)\delta(M_R^2-m_S^2).\end{aligned} \tag{3.12}$$

The inclusive differential cross section is obtained in a factorized form:

$$\frac{d\sigma^{\rm inc}(p(\gamma)p(\gamma)\to S+X)}{dy_S} = \frac{8\pi^2\Gamma(S\to\gamma\gamma)}{m_S}\times\left.\frac{d\mathcal{L}^{\rm inc}_{\gamma\gamma}}{dM_R^2\,dy_S}\right|_{M_R=m_S}. \tag{3.13}$$

Now taking the values for $\gamma(x,\mu)$ in Ref. [184], we obtain a convenient form of cross section

$$\sigma^{\rm inc}(p(\gamma)p(\gamma)\to S+X) = 91\,{\rm fb}\left(\frac{\Gamma_{\rm tot}(S)}{1\,{\rm GeV}}\right)\mathcal{B}(S\to\gamma\gamma), \tag{3.14}$$

or

$$\sigma^{\rm inc}(p(\gamma)p(\gamma)\to S+X\to\gamma\gamma+X) = 91\,{\rm fb}\left(\frac{\Gamma_{\rm tot}(S)}{1\,{\rm GeV}}\right)\mathcal{B}^2(S\to\gamma\gamma), \tag{3.15}$$

for evaluating production cross sections at $\sqrt{s}=13\,{\rm TeV}$. The reference magnitude of the cross section, 91 fb, is much greater than that in [40] obtained under the narrow width approximation and effective photon approximation [208, 209], $1.6-3.6\,{\rm fb}$ (depending on the minimum impact

[5] See also [13, 120, 154, 157, 159, 186–207] for related issues.

Final state	Upper bound (in fb, 95% C.L.)	Category	Ref.
$\gamma\gamma$	2.4/2.4	8TeV-ATLAS/CMS	[126, 127]
	13/13	13TeV-ATLAS/CMS	[3, 4]
$Z\gamma$	4.0/27	8TeV/13TeV-ATLAS	[210, 211]
ZZ	12/99	8TeV/13TeV-ATLAS	[130, 212]
WW	35	8TeV-ATLAS	[213]
hh	40	8TeV-ATLAS	[214]

Table 2: 95% C.L. upper bounds on decay channels of a 750 GeV scalar resonance.

parameter for elastic scattering), while it is smaller than that in [187] through a similar calculation with in [184], 240 fb. We also find at $M_R = 750\,\text{GeV}$ in Ref. [184]

$$\frac{\mathcal{L}^{\text{inc}}_{\gamma\gamma}(\sqrt{s} = 13\,\text{TeV})}{\mathcal{L}^{\text{inc}}_{\gamma\gamma}(\sqrt{s} = 8\,\text{TeV})} \approx 2.9. \tag{3.16}$$

Having the above relations in Eqs. (3.14)-(3.16), it is straightforward to evaluate the inclusive production cross section at $\sqrt{s} = 8\,\text{TeV}$. We note that the resultant value is greater than the value (≈ 2) cited in Ref. [187].

3.2 Results

3.2.1 Case 1: without mass mixing

In this part, we discuss the case that the field S is a mass eigenstate, where no mixing effect is present through mass terms with other scalars. Under our assumptions, the relevant parameters are $(m_{k^{\pm\pm}}, \mu_{Sk}, N_j)$: the universal physical mass of the doubly charged scalars (assuming $m_{k^{\pm\pm}} = m_{j_a^{\pm\pm}}$ for all a), the universal effective scalar trilinear coupling (assuming $\mu_{Sk} = \mu_{Sj_a}$ for all a), and the number of the additional doubly charged singlet scalars. We observe the unique relation among the branching ratios of S irrespective of $m_{k^{\pm\pm}}$ and μ_{Sk}, which is suggested by Eq. (3.1), as

$$\mathcal{B}(S \to \gamma\gamma) \simeq 0.591, \quad \mathcal{B}(S \to \gamma Z) \simeq 0.355, \quad \mathcal{B}(S \to ZZ) \simeq 0.0535. \tag{3.17}$$

In Ref. [215], reasonable target values for the cross section of $\sigma_{\gamma\gamma} \equiv \sigma(pp \to S + X \to \gamma\gamma + X)$ at the $\sqrt{s} = 13\,\text{TeV}$ LHC were discussed as functions of the variable $R_{13/8}$, which is defied as

$$R_{13/8} \equiv \frac{\sigma(pp \to S)|_{\sqrt{s}=13\,\text{TeV}}}{\sigma(pp \to S)|_{\sqrt{s}=8\,\text{TeV}}}, \tag{3.18}$$

where the published data after Moriond 2016 are included, and the four categories discriminated by the two features (spin-0 or spin-2; narrow width $[\Gamma_S/m_S \to 0]$ or wide width $[\Gamma_S/m_S = 6\%]$) are individually investigated. As pointed out in Eq. (3.17), the value of $\mathcal{B}(S \to \gamma\gamma)$ is uniquely fixed as $\simeq 60\%$ and S is produced only through the photon fusion in the present case. As shown in Eq. (3.16) in our estimation of the photo-production, $R_{13/8}$ corresponds to 2.9, where the best fit values of $\sigma_{\gamma\gamma}$ at $\sqrt{s} = 13\,\text{TeV}$ are extracted from [215] as

$$2.0 \pm 0.5\,\text{fb} \quad (\text{for } \Gamma_S/m_S \to 0), \qquad 4.25 \pm 1.0\,\text{fb} \quad (\text{for } \Gamma_S/m_S = 6\%). \tag{3.19}$$

The theoretical error in the present formulation of the photo-production was evaluated as $\pm 15-20\%$ in [184]. Then, we decide to focus on the 2σ favored regions with including the error (20%, fixed) also, concretely speaking,

$$[0.8, 3.6]\,\text{fb} \quad (\text{for } \Gamma_S/m_S \to 0), \qquad [1.8, 7.5]\,\text{fb} \quad (\text{for } \Gamma_S/m_S = 6\%). \tag{3.20}$$

Here, the 95% CL upper bound on $\sigma_{\gamma\gamma}$ at $\sqrt{s} = 8\,\text{TeV}$ is $\lesssim 2.4\,\text{fb}$ [126, 127] and the favored regions are still consistent with the 8 TeV result (or just on the edge). It is found that the bounds on the $Z\gamma$, ZZ final states are weaker than that of $\gamma\gamma$. Relevant information is summarized in Table 2.

In Fig. 2, situations in our model are summarized. Six cases with different numbers of doubly charged scalars are considered with $N_j = 0, 1, 10, 100, 200$ and 300. Here, we should mention an important issue. As indicated in Fig. 2, when N_j is zero, more than $10 \sim 20\,\text{TeV}$ is required in the effective trilinear coupling μ_{Sk}. Such a large trilinear coupling would immediately lead to the violation of tree level unitarity in the scattering amplitudes including μ_{Sk}, e.g., $k^{++}k^{--} \to k^{++}k^{--}$ or $SS \to k^{++}k^{--}$ at around the energy 1 TeV, where the physics with our interest is spread. Also, the vacuum is possibly threatened by the destabilization via the large trilinear coupling, which calls charge breaking minima. To evade the problems, naively speaking, the value of μ_{Sk} is less than $1 \sim 5\,\text{TeV}$.[6]

Also, we consider the doubly charged singlet scalars produced via $pp \to \gamma^*/Z + X \to k^{++}k^{--} + X$. Lower bounds at 95% C.L. on $m_{k^{\pm\pm}}$ via the 8 TeV LHC data were provided by the ATLAS group in Ref. [217] as 374 GeV, 402 GeV, 438 GeV when assuming a 100% branching ratio to $e^\pm e^\pm$, $e^\pm\mu^\pm$, $\mu^\pm\mu^\pm$ pairs, respectively. In our model, the doubly charged scalars can decay through the processes as shown in Fig. 3, where h_1^+'s are off shell since it should be heavy at least 3 TeV. In the case of k^{++} in $N_j = 0$, when the values of μ_{11} and μ_{22} are the same or similar, from Eq. (2.2), the relative branching ratios between $k^{++} \to \mu^+\mu^+\nu_i\nu_j$ and $k^{++} \to \mu^+\mu^+$ are roughly proportional to $(y_L)_{2i}(y_L)_{2j}$ and $((y_R)_{22})^2$. As concluded in our previous work [150], the absolute value of $(y_R)_{22}$ should be large as around $8 \sim 9$ to generate the observed neutrino properties, while a typical magnitude of $(y_L)_{2i}$ is $0.5 \sim 1$. Then, the decay branch $k^{++} \to \mu^+\mu^+$ is probably dominant as $\sim 100\%$ and we need to consider the 8 TeV bound seriously. A simplest attitude would be to avoid to examine the shaded regions in Fig. 2, which indicate the excluded parts in 95% C.L. via the ATLAS 8 TeV data with the assumption of $\mathcal{B}(k^{\pm\pm} \to \mu^\pm\mu^\pm) = 100\%$ [217].

[6] In the case of MSSM with a light $\tilde{t}_1$ (100 GeV), $A = A_t = A_b$, $\tan\beta \gg 1$, $m_A \gg M_Z$, $|\mu| \ll M_{\tilde{Q}}$ and $M_{\tilde{b}}$, the bound on the trilinear coupling $|A| \lesssim 5\,\text{TeV}$ was reported in Ref. [216].

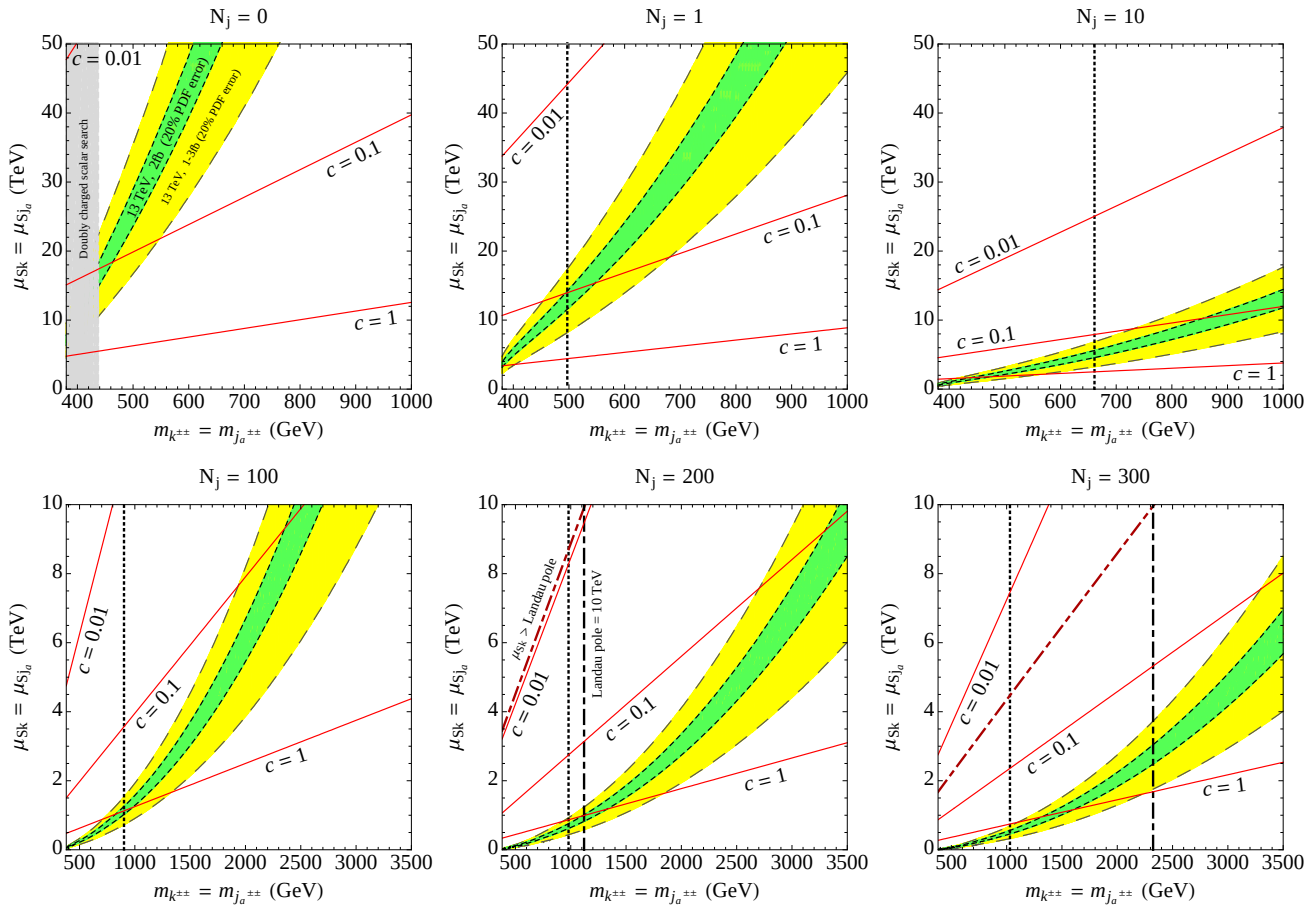

Figure 2: Six cases with different numbers of doubly charged scalars are considered with $N_j = 0, 1, 10, 100, 200$ and 300. Inside the green regions, the best fit value of the production cross section is realized with taking account of $\pm 20\%$ theoretical error discussed in [184]. The yellow regions indicate the areas where we obtain the 2σ-favored values in the production cross section of $p(\gamma)p(\gamma) \to S + X \to \gamma\gamma + X$, where we take account of both of the theoretical ($\pm 20\%$) and experimental (shown in Eq. (3.19)) errors. Cross section evaluations are owing to Eq. (3.15). The gray shaded region $m_{k^{\pm\pm}} \leq 438\,\mathrm{GeV}$ in $N_j = 0$ shows the excluded parts in 95% C.L. via the ATLAS 8 TeV search for doubly charged particles with the assumption of $\mathcal{B}(k^{\pm\pm} \to \mu^\pm\mu^\pm) = 100\%$ [217]. The vertical black dotted lines represent corresponding bounds on the universal physical mass $m_{k^{\pm\pm}}$ when we assume $\mathcal{B}(j_a^{\pm\pm} \to \mu^\pm\mu^\pm) = 100\%$ for all $j_a^{\pm\pm}$. Two types of constraints with respect to "Landau pole" of g_Y (defined as $g_Y(\mu) = 4\pi$) are meaningful when N_j is large ($N_j = 200$, 300). The red lines indicate three reference boundaries of the correction factor $c\,\delta = 1$ with $c = 1$, 0.1, 0.01 to the trilinear couplings μ_{Sk} ($= \mu_{Sj_a}$) defined in Eq. (3.22). For each choice of c, the region below the corresponding boundary is favored from a viewpoint of perturbativity.

When one more doubly charged scalar j_1^{++} ($N_j = 1$) exists, a detailed analysis is needed for precise bounds on $k^{\pm\pm}$ and $j_1^{\pm\pm}$. Benchmark values are given in Fig. 2 by the vertical black dotted lines, which represent corresponding bounds on the universal physical mass $m_{k^{\pm\pm}}$ when we assume $\mathcal{B}(j_a^{\pm\pm} \to \mu^\pm\mu^\pm) = 100\%$ for all $j_a^{\pm\pm}$. We obtain the 95% C.L. lower bounds on the universal mass value $m_{k^{\pm\pm}}$ as $\sim 500\,\mathrm{GeV}$ ($N_j = 1$), $\sim 660\,\mathrm{GeV}$ ($N_j = 10$), $\sim 900\,\mathrm{GeV}$ ($N_j = 100$), $\sim 980\,\mathrm{GeV}$ ($N_j = 200$), and $\sim 1030\,\mathrm{GeV}$ ($N_j = 300$), respectively through the numerical simulations by `MadGraph5_aMC@NLO` [218, 219] with the help of `FeynRules` [220–222] for model implementation.

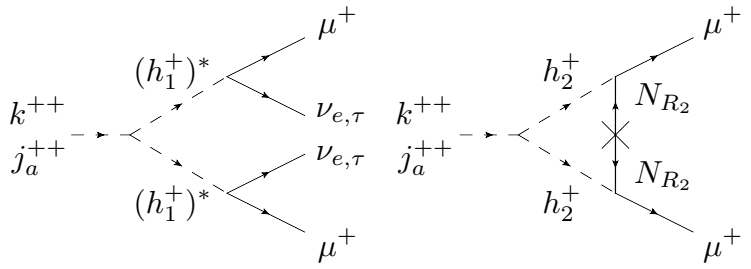

Figure 3: A schematic description for the decay patterns of k^{++} or j_a^{++} with two anti-muons in the final state. Here, h_1^+'s in the left diagram are off-shell particles.

The method which we adopt for evaluating the corresponding 95% C.L. bounds with the assumption of $\mathcal{B}(j_a^{\pm\pm} \to \mu^\pm\mu^\pm) = 100\%$ for all $j_a^{\pm\pm}$, where more than one doubly charged scalars exist, is as follows. When N number of doubly charged scalars are present, the expected number of the total signal receives the multiplicative factor N. Following this statement, we can estimate the bound on the universal mass $m_{k^{\pm\pm}}$ via the pair production cross section of a doubly charged scalar $k^{\pm\pm}$ (in $N = 1$ case) though the sequence $pp \to \gamma^*/Z + X \to k^{++}k^{--} + X$. The bound should correspond to the mass where the production cross section is N-times smaller than the benchmark value in $m_{k^{\pm\pm}} = 438\,\mathrm{GeV}$, which is the 95% C.L lower bound on $m_{k^{\pm\pm}}$ form the ATLAS 8 TeV data [217]. We obtained the leading order cross section as 0.327 fb, which is fairly close to the ATLAS value, 0.357 fb read from Fig. 4 (c) of Ref. [217]. In calculation, we used `CTEQ6L` proton PDF [223] and set the renormalization and factorization scales as $2m_{k^{\pm\pm}}$.

Here, we point out an interesting possibility. From Eq. (2.9), if $\lambda_{11}^{(1)}\langle\Sigma_0^*\rangle$ is quite larger than $\mu_{22}^{(1)}$, the pattern $j_1^{++} \to \mu^+\mu^+\nu_i\nu_j$ possibly becomes considerable, where we cannot reconstruct the invariant mass of the doubly charged scalar since missing energy exists in this decay sequence. Then, significance for exclusion would be dropped and we could relax the bound on $m_{j_1^{\pm\pm}}$ to some extent. An extreme case is with a nonzero $\lambda_{11}^{(1)}\langle\Sigma_0^*\rangle$ and $\mu_{22}^{(1)} = 0$, where the branching ratio of $j_1^{++} \to \mu^+\mu^+$ becomes zero at the one loop level and the significance takes the lowest value, which is the best for evading the 8 TeV LHC bound. Also in this situation, no additional contribution to the neutrino mass matrix exists and the original successful structure is not destroyed. Similar discussions are applicable when N_j is more than one.

When we assume 100% branching fractions in $j_a^{++} \to \mu^+\mu^+$ for all j_a^{++}, the common trilinear coupling μ_{Sk} should be larger than $\sim 10\,\mathrm{TeV}$ ($N_j = 0$), $\sim 8\,\mathrm{TeV}$ ($N_j = 1$), $\sim 3\,\mathrm{TeV}$ ($N_j = 10$), less than 1 TeV ($N_j = 100$, 200, 300), to obtain a reasonable amount of the production cross section with taking into account of the $\pm 20\%$ theoretical error in cross section as suggested by Fig. 2. As mentioned, large trilinear couplings $\lambda_{11}^{(a)}\langle\Sigma_0^*\rangle$ can help us to alleviate the 8 TeV bound.

Another theoretical bound is reasonably expected when, as in the present situation, many new particles with nonzero gauge charges are introduced around 1 TeV. The presence of multiple doubly charged $SU(2)_L$ singlet scalars deforms the energy evolution of the $U(1)_Y$ gauge coupling g_Y as

$$\frac{1}{g_Y^2(\mu)} = \frac{1}{g_Y^2(m_{\rm input})} - \frac{b_Y^{\rm SM}}{16\pi^2}\log\left(\frac{\mu^2}{m_{\rm input}^2}\right) - \theta(\mu - m_{\rm threshold})\frac{\Delta b_Y}{16\pi^2}\log\left(\frac{\mu^2}{m_{\rm threshold}^2}\right), \qquad (3.21)$$

where $b_Y^{\rm SM} = 41/6$, $\Delta b_Y = 4/3(N_j + 1)$, and we implicitly assume the relation $m_{\rm input}\,(= m_Z) < m_{\rm threshold}\,(= m_{k^{\pm\pm}} = m_{j_a^{\pm\pm}})$. As a reasonable criterion, we require that the theory is still not

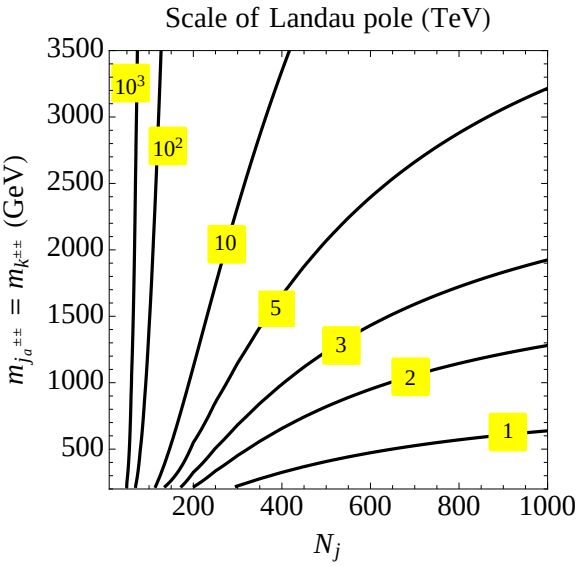

Figure 4: Positions of "Landau pole" defined as $g_Y(\mu) = 4\pi$

drastically strongly-coupled within the LHC reach $\sim$ 10 TeV.[7] Positions of "Landau pole" μ, which is defined as $g_Y(\mu) = 4\pi$, are calculated with ease as functions of N_j and $m_{\rm threshold}$ $(= m_{k^{\pm\pm}} = m_{j_a^{\pm\pm}})$ as shown in Fig. 4. Now, we recognize that under the criterion, the case with $N_j \lesssim 100$ is not restricted in the sense that the bound via the "Landau pole" is much weaker than the phenomenological requirement $m_{k^{\pm\pm}}$ $(= m_{j_a^{\pm\pm}}) \gtrsim 375\,{\rm GeV}$ (for preventing the decays $S \to k^{++}k^{--}$, $j_a^{++}j_a^{--}$). On the other hand when N_j is rather larger than 100, meaningful bounds are expected from Fig. 4. For example, when $N_j = 200$ (300), $m_{k^{\pm\pm}}$ $(= m_{j_a^{\pm\pm}})$ should be greater than $\sim 1.1\,{\rm TeV}$ ($\sim 2.2\,{\rm TeV}$).

There also arises a largish loop contribution to the universal trilinear coupling μ_{Sk} $(= \mu_{Sj_a})$ as

$$\mu_{Sk} \to \mu_{Sk}\,(1 + c\,\delta), \quad \delta = \frac{N_j + 1}{16\pi^2} \times \left(\frac{\mu_{Sk}}{m_{k^{\pm\pm}}}\right)^2 . \tag{3.22}$$

A convenient parameter, $c \lesssim 1$, encapsulates the effects from all higher order contributions. Precise determination of c is beyond the scope of this paper thus, instead, we show the cases with $c = 0.01, 0.1$ and 1 as benchmarks (see Fig 2). It is easily noticed that the loop-induced value could dominate over the tree level value unless $c\,\delta < 1$, or equivalently $\mu_{Sk}/m_{k^{\pm\pm}} < 4\pi/\sqrt{c\,(N_j + 1)}$. This may affect the convergence of the multi-loop expansion even though the theory is still renormalizable.[8]

Unfortunately when N_j is only a few, explaining the diphoton excess is not consistent since the value of μ_{Sk} is too large and tree level unitarity is violated. This problem is avoided when $N_j \gtrsim 10$, whereas the evolution of g_Y through renormalization group effect puts additional bounds on $m_{k^{\pm\pm}}$ $(= m_{j_a^{\pm\pm}})$ when $N_j \gtrsim 100$. The preferred parameter would be further constrained by

[7] We note that measurements of running electroweak couplings put bounds on additional contributions to the beta functions of the $SU(2)_L$ and $U(1)_Y$ gauge couplings [224] even though the work [224] did not survey the parameter range which is relevant for our discussion. Similar discussions have been done in the QCD coupling [225, 226], which is basically irrelevant in our case.

[8] One should note, however, that $c\,\delta < 1$ is not absolute requirement for a consistent theory. See e.g. [227] where a loop-induced value overwhelms the tree-level counterpart in the context of two Higgs doublet model.

$c\,\delta < 1$ as in Fig. 2. In conclusion, we can explain the 750 GeV excess consistently even when $\mathcal{B}(j_a^{\pm\pm} \to \mu^\pm\mu^\pm) = 100\%$ for all $j_a^{\pm\pm}$.

3.2.2 Case 2: with mass mixing

In this section, we investigate the situation when the mass mixing between S and Φ are allowed. At first, we phenomenologically introduce the mixing angle β as,

$$\begin{pmatrix}\phi\\ S\end{pmatrix} = \begin{pmatrix}c_\beta & s_\beta\\ -s_\beta & c_\beta\end{pmatrix}\begin{pmatrix}h\\ S'\end{pmatrix}, \tag{3.23}$$

where we use the short-hand notations, $c_\beta \equiv \cos\beta$, $s_\beta \equiv \sin\beta$, and express the observed 125 GeV and 750 GeV scalars (mass eigenstates) by h and S', respectively. We assume the following effective interactions among scalars

$$\Delta\mathcal{V}_{\rm eff} = \frac{1}{2}m_h^2h^2 + \frac{1}{2}m_{S'}^2S'^2 + \mu_{Sk}S|k^{++}|^2 + \mu_{Sj_a}S|j_a^{++}|^2 + \hat{\mu}_{S\Phi}S|\Phi|^2 + \hat{\lambda}_{S\Phi}S^2|\Phi|^2, \tag{3.24}$$

where m_h and $m_{S'}$ represent the mass eigenvalues 125 GeV and 750 GeV; μ_{Sk} and μ_{Sj_a} are effective trilinear couplings as defined in Eq. (2.10), where the contents of them are not important in this study. We note that we safely ignore the terms $\phi|k^{++}|^2$ and $\phi|j_a^{++}|^2$ since these terms originate from the gauge-invariant interactions $|\Phi|^2|k^{++}|^2$ and $|\Phi|^2|j_a^{++}|^2$, where effective trilinear couplings of them are small compared with μ_{Sk} and μ_{Sj_a}. Because of the mixing in Eq. (3.23), the terms $h|k^{++}|$ and $h|j_a^{++}|$ are induced and can affect the signal strength of h.

The S'-h-h interaction may be also introduced via the interaction Lagrangian:

$$\frac{1}{2}\mu_{S'h}S'h^2 \quad \text{with} \quad \mu_{S'h} \equiv m_{S'h}\left[c_\beta^3 - 2c_\beta s_\beta^2\right], \tag{3.25}$$

where $m_{S'h}$ represents a mass scale and the mixing factor could be determined via the gauge invariant term $S|\Phi|^2$.[9]

A signifiant distinction from the previous no-mixing case is that the 750 GeV scalar can couple to the SM particles through the mixing effect. The inclusive production cross section at the LHC is deformed as

$$\sigma(pp \to S' + X) \simeq (\sigma^{\rm ggF}_{pp\to H^{\rm SM}_{750\,\rm GeV}} + \sigma^{\rm VBF}_{pp\to H^{\rm SM}_{750\,\rm GeV}})s_\beta^2 + \sigma^{\rm pf}_{pp\to S'}, \tag{3.27}$$

where $\sigma^{\rm ggF}_{pp\to H^{\rm SM}_{750\,\rm GeV}}$ and $\sigma^{\rm VBF}_{pp\to H^{\rm SM}_{750\,\rm GeV}}$ represent the inclusive production cross section of the SM-like Higgs boson with 750 GeV mass through the gluon fusion and vector boson fusion processes, respectively. $\sigma^{\rm pf}_{pp\to S'}$ shows a corresponding value through the photon fusion in Eq. (3.14). We adopt the following digits in [91, 129, 228, 229],

$$\sigma^{\rm ggF}_{pp\to H^{\rm SM}_{750\,\rm GeV}} = \begin{cases}156.8\,\text{fb} & \text{at } \sqrt{s} = 8\,\text{TeV}\\ 590\,\text{fb} & \text{at } \sqrt{s} = 13\,\text{TeV}\end{cases}, \quad \sigma^{\rm VBF}_{pp\to H^{\rm SM}_{750\,\rm GeV}} = \begin{cases}50\,\text{fb} & \text{at } \sqrt{s} = 8\,\text{TeV}\\ 220\,\text{fb} & \text{at } \sqrt{s} = 13\,\text{TeV}\end{cases}, \tag{3.28}$$

$$\Gamma_{\rm tot}(H^{\rm SM}_{750\,\rm GeV}) = 247\,\text{GeV}, \quad \mathcal{B}(H^{\rm SM}_{750\,\rm GeV} \to WW) = 58.6\%, \quad \mathcal{B}(H^{\rm SM}_{750\,\rm GeV} \to ZZ) = 29.0\%. \tag{3.29}$$

[9] When $\langle S\rangle = 0$, the scale of $m_{S'h}$ is determined through the two mass eigenvalues and the mixing angle β as

$$m_{S'h} = \left(\frac{m_{S'}^2 - m_h^2}{v}\right)\sin(2\beta), \tag{3.26}$$

since the mass mixing term $S\phi$ and the three point vertex $S\phi^2$ have the unique common origin $S|\Phi|^2$. Plots in this situation are provided in Appendix C.

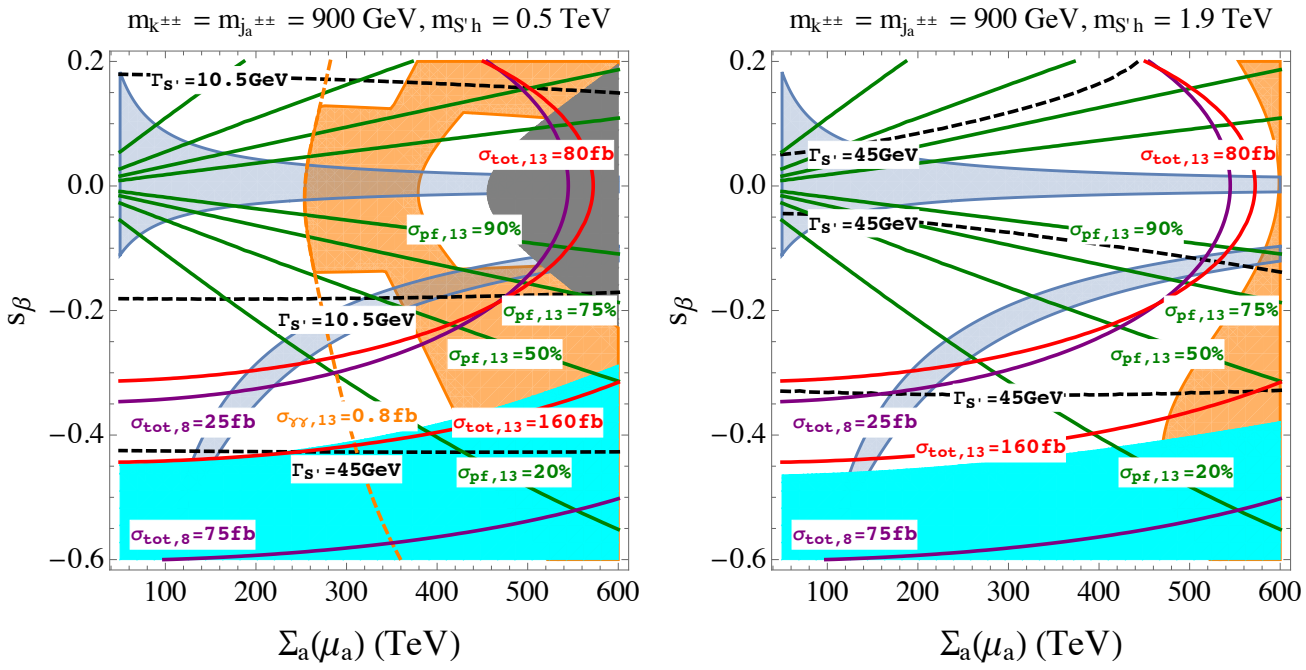

Figure 5: Allowed ranges of the parameters $\{\sum_a(\mu_a), s_\beta\}$ are shown in the choice of the mass of the degenerated doubly charged scalars ($m_{k^{\pm\pm}}$ [$= m_{j_a^{\pm\pm}}$] $= 900\,\text{GeV}$) and two different choices of $m_{S'h}$ (0.5 TeV [left panel] and 1.9 TeV [right panel]). The light blue regions represent 2σ allowed regions of 125 GeV Higgs signal strengths, while the orange regions suggest the areas where the 750 GeV excess is suitably explained. The gray/cyan regions are excluded in 95% C.L.s by the ATLAS 8 TeV results for $S' \to \gamma\gamma/ZZ$. For better understanding, several contours for the total width of S' ($\Gamma_{S'}$), total production cross sections at $\sqrt{s} = 8/13\,\text{TeV}$ ($\sigma_{\text{tot},8/13}$), and the percentage of the production through the photon fusion at $\sqrt{s} = 13\,\text{TeV}$ ($\sigma_{\text{pf},13}$) are illustrated.

Part of relevant partial decay widths are written down as

$$\Gamma_{S'\to WW} = \Gamma_{H^{\text{SM}}_{750\,\text{GeV}}\to WW}\, s_\beta^2, \tag{3.30}$$

$$\Gamma_{S'\to hh} \sim \frac{(\mu_{S'h})^2}{32\pi m_{S'}}\sqrt{1-\frac{4m_h^2}{m_{S'}^2}}, \tag{3.31}$$

The total width takes the form

$$\Gamma_{\text{tot}}(S') \sim \left[\Gamma_{\text{tot}}(H^{\text{SM}}_{750\,\text{GeV}}) - \Gamma_{H^{\text{SM}}_{750\,\text{GeV}}\to ZZ}\right] s_\beta^2 + \Gamma_{S'\to\gamma\gamma} + \Gamma_{S'\to Z\gamma} + \Gamma_{S'\to ZZ} + \Gamma_{S'\to hh}, \tag{3.32}$$

where the minuscule parts $\mathcal{B}(H^{\text{SM}}_{750\,\text{GeV}} \to \gamma\gamma) = 1.79\times10^{-5}\%$, $\mathcal{B}(H^{\text{SM}}_{750\,\text{GeV}} \to Z\gamma) = 1.69\times10^{-4}\%$, and $\mathcal{B}(H^{\text{SM}}_{750\,\text{GeV}} \to gg) = 2.55\times10^{-2}\%$ [129] could be safely neglected. Here, $\Gamma_{S'\to\gamma\gamma}$, $\Gamma_{S'\to Z\gamma}$ and $\Gamma_{S'\to ZZ}$ describe decay widths at one loop level, where the multiple doubly charged scalars propagating in the loops. When we take the limit $s_\beta \to 0$, they are reduced to Eqs. (3.2)-(3.4). Explicit forms of these widths are summarized in Appendix B.

In Fig. 5, prospects are widely discussed in the choice of the mass of the degenerated doubly charged scalars ($m_{k^{\pm\pm}}$ [$= m_{j_a^{\pm\pm}}$] $= 900\,\text{GeV}$) and two different choices of $m_{S'h}$ (0.5 TeV [left panel] and 1.9 TeV [right panel]). First, we emphasize that the 125 GeV Higgs h couples to the doubly

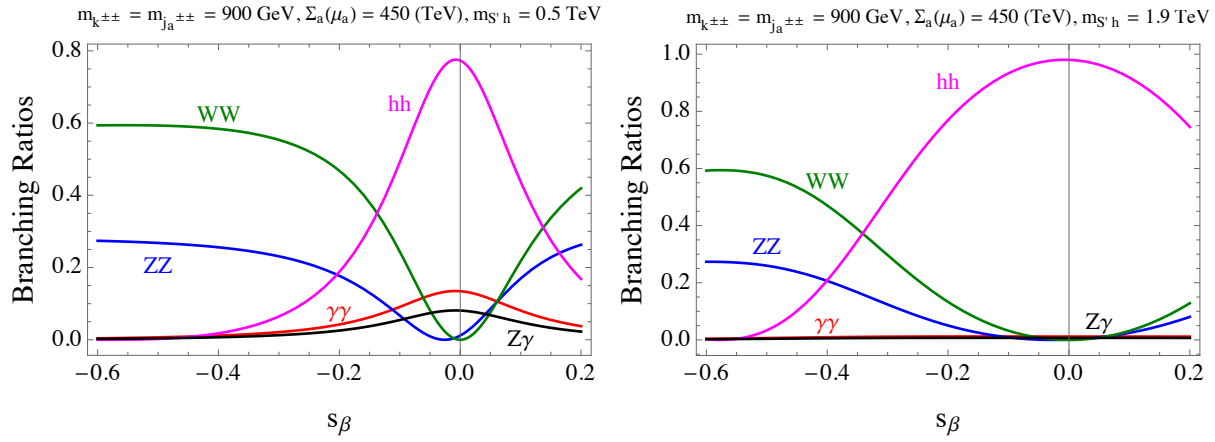

Figure 6: Relevant branching ratios of S' in the two configurations in Fig. 5 are shown. Here, values of $\Sigma_a(\mu_a)$ are suitably fixed as typical digits in the corresponding allowed regions.

charged scalars through the mixing in Eq. (3.23) in the present setup. As in Ref. [150], we take the results at $\sqrt{s} = 7$ and 8 TeV of the five Higgs decay channels reported by the ATLAS and the CMS experiments into consideration, which are $h \to \gamma\gamma$, $h \to ZZ$, $h \to WW$, $h \to b\bar{b}$, $h \to \tau^+\tau^-$ [230–235], and calculate a χ^2 variables for estimating 2σ allowed ranges of the parameter space, which are depicted in light blue color.[10] Here, we find two types of allowed regions with and without including $s_\beta = 0$, which correspond to the cases with and without accidental cancellation between SM contributions and the new contributions through the mixing, respectively.

The orange regions suggest the 2σ-favored areas with taking account of the 20% theoretical error in the present way for photon-fusion production cross section summarized in Eq. (3.20). Here, we use the values in the cases of $\Gamma/m \to 0$ and $\Gamma/m = 6\%$ for the regions $\Gamma/m < 1\%$ and $\Gamma/m \geq 1\%$ for an illustration, respectively. The gray/cyan regions are excluded in 95% C.L.s by the ATLAS 8 TeV results for $S' \to \gamma\gamma/ZZ$. For better understanding, several contours for the total width of S' ($\Gamma_{S'}$), total production cross sections at $\sqrt{s} = 8/13$ TeV ($\sigma_{\mathrm{tot},8/13}$), and the percentage of the production through the photon fusion at $\sqrt{s} = 13$ TeV ($\sigma_{\mathrm{pf},13}$) are illustrated. Relevant branching ratios of S' are shown in Fig. 6 for the two configurations in Fig. 5.

Now, we focus on two types of consistent solutions around $s_\beta \simeq 0$ and $s_\beta \simeq -0.15$. Physics in the situation $s_\beta \simeq 0$ is basically the same with the previous "Case 1" without mass mixing effect, where the total decay width is small, concretely less than 1 GeV. On the other hand when $s_\beta \simeq -0.15$, partial widths of decay branches which are opened by a nonzero value of s_β become sizable and expected values of the total width can become, interestingly, near 10.5 GeV or 45 GeV, which are the latest 13 TeV best fit value of the CMS and ATLAS group, respectively.

Finally, we briefly comment on tree level unitarity. When we consider $m_{k^{\pm\pm}}$ [$= m_{j_a^{\pm\pm}}$] = 900 GeV, the bound via tree level unitarity is relaxed in both of $s_\beta \simeq 0$ and $s_\beta \simeq -0.15$. However, with a large value of the universal trilinear coupling in 3 to 6 TeV range, $c\,\delta < 1$ is achieved only if $c \ll 1$ when $\mathcal{B}(j_a^{\pm\pm} \to \mu^\pm\mu^\pm) = 100\%$ for all $j_a^{\pm\pm}$, which may requests further model building efforts.

[10] The original model contains invisible channels in the 125 GeV Higgs boson due to the existence of a dark matter candidate and a Nambu-Goldstone boson from the spontaneous breaking of a global $U(1)$. We ignore the invisible widths in the global fit for simplicity.

4 Conclusion and discussion

In this paper, we investigated a possibility for explaining the recently announced 750 GeV diphoton excess by the ATLAS and the CMS experiments at the CERN LHC in the context of loop induced singlet production and decay through photon fusion. When a singlet scalar S, which is a candidate of the resonance particle, couples to doubly charged particles, we can obtain a suitable amount of the cross section of $pp \to S + X \to \gamma\gamma + X$ without introducing a tree-level production of S. In three-loop radiative neutrino models, $SU(2)_L$ singlet multiple doubly charged scalars are introduced such that the S-γ-γ vertex is radiatively generated and enhanced. When we consider such type of doubly charged scalar(s), the branching ratio $\mathcal{B}(S \to \gamma\gamma)$ is uniquely fixed as $\simeq 60\%$ by quantum numbers when S is a mass eigenstate. Constraints from 8 TeV LHC data are all satisfied.

A fascinating feature in the single S production through photon fusion is that the value of $\mathcal{B}(S \to \gamma\gamma)$ as well as Γ_S determines the production cross section, as shown in Eqs. (3.14) and (3.15). With the branching fraction to diphoton $S \to \gamma\gamma \simeq 60\%$ (see Sec. 3.2.1), when we take 'wide width' scenario with $\Gamma/m \sim 6\%$, the expected cross section to diphton is too large. However, in 'narrow width scenario' with $\Gamma_S = 62.9\,\text{MeV}$, it is nicely fit to the best fit value for the inclusive cross section of 2 fb. We also note that the width is close to the $8+13$ TeV best-fit value announced by the CMS group (105 MeV) [see App. C]. This is an informative prediction of our present scenario which should be tested in the near future. Also the relative strengths of the one loop induced partial decay widths are insensitive to N_j as shown in Eq. (3.1) when the mixing effect between S and the Higgs doublet Φ is negligible. This universality is a remarkable property of our scenario and this relation can be tested when more data would be available.

When S and the Higgs doublet Φ can mix, some distinctive and interesting features are found. In the first thought, only a small mixing $\sin\beta \ll 1$ is allowed to circumvent drastic modifications to 125 GeV Higgs signal strengths but we could see another interesting region of parameter space with $\sin\beta \simeq -0.15$, where the 750 GeV excess can be explained consistently within 'wide width' scenario (see Sec. 3.2.2). However a big part of the parameter space, especially in the case with the scalar mixing, would lie outside of $c\,\delta < 1$ region, which requires $c \ll 1$ for a viable model.

Finally, we discuss further extensions of the model and other phenomenological issues.

- A possible extension of the present direction is to introduce N_S number of $SU(2)_L$ singlet scalars, $(S = S_1, S_2, \cdots, S_{N_S})$, without hypercharge in the theory. If the masses of the scalars are almost degenerate to 750 GeV, the current experiment may not be able to detect the multi bumps so that they would look as a single bump as we face. The total cross section, then, is enhanced by the multiplicative factor of N_S^2 as

$$\sigma_{\text{tot}}(pp \to \gamma\gamma + X) \approx N_S^2 \sigma(pp \to S + X \to \gamma\gamma + X). \tag{4.1}$$

- Another possible extension is that we also introduce the singly charged scalars $\tilde{h}^\pm_{1,2}$ which hold the same quantum numbers as $h^\pm_{1,2}$ and has the same interaction with $j_a^{\pm\pm}$ as $h^\pm_{1,2}$ do with $k^{\pm\pm}$. In such a possibility, contributions to the neutrino mass matrix are enhanced and we can reduce the value of the large coupling required for a consistent explanation in the original model, especially in $(y_R)_{22}$. See Appendix for details.

- The triple coupling of the Higgs boson could be enhanced in our case that may activate the strong first order phase transition, which is a necessity for realizing the electroweak baryogenesis scenario [236]. In such a case, radiative seesaw models can explain not only neutrino mass and dark matter but also baryon asymmetry of the Universe.

- The decays $k^{\pm\pm} \to \ell^\pm\ell^\pm$ and $j_a^{\pm\pm} \to \ell^\pm\ell^\pm$ provide very clean signatures. The 13 TeV LHC would be expected to replace the current bound on the universal mass, e.g., $m_{k^{\pm\pm}} > 438\,\text{GeV}$ when $\mathcal{B}(k^\pm/j_a^\pm \to \mu^\pm\mu^\pm) = 100\%$ for all the doubly charged scalars, from the 8 TeV data [217] soon. An important feature recognized from Fig. 2 is that when N_j is not so large as around 10, only light doubly charged scalars are consistent with the bound from tree level unitarity. Such possibilities would be exhaustively surveyed and eventually confirmed or excluded in the near future. On the other hand, when N_j is large as around 10, from Fig. 2, more than $\sim 700\,\text{GeV}$ doubly charged scalars can exist with holding tree level unitarity. Such heavy particles require a suitable amount of integrated luminosity for being tested in colliders. In other words, such possibilities are hard to be discarded in the near future.

- It might be worth mentioning the discrimination between our model discussed here and the other well known radiative models, namely, Zee model [131] at the one-loop level, Zee-Babu model [133, 134] at the two-loop level, Kraus-Nasri-Trodden (KNT) model [136], Aoki-Kanemura-Seto (AKS) model [137, 138], and Gustafsson-No-Rivera (GNR) model [139] at the three-loop level. Essentially, any model that includes isospin singlet charged bosons potentially explain the 750 GeV diphoton excess along the same way as discussed in this paper. Among those, three-loop models have natural DM candidates by construction, which we regard as a phenomenological big advantage. Our model shares this virtue. On the other hand, in view of the charged-boson, our model and also the GNR model include doubly charged particles. From the currently available data, it is not possible to distinguish the effect of a singly charged scalar from a double charged scalar. However, we still see that a doubly charged boson is in favor of the explanation of the 750 GeV diphoton excess simply because of the enhanced diphoton coupling.

- As we discussed before, $k^{\pm\pm}$ decays to $\mu^\pm\mu^\pm$ with an almost 100% branching fraction, distinctively from other models, e.g., Zee-Babu model, due to the large coupling $(y_R)_{22} \gtrsim 2\pi$, which is required to realize the observed neutrino data in our setup consistently.

Note Added: In the recent update in ICHEP 2016 (on 5th August 2016) after we submitted this manuscript to PTEP, which includes the analyzed data accumulated in 2016 (ATLAS: $15.4\,\text{fb}^{-1}$, CMS: $12.9\,\text{fb}^{-1}$), the 750 GeV diphoton signal now turns out to be statistically disfavored [237, 238]. Nevertheless, we are still motivated to study the diboson resonance which may show up in a higher energy domain[11] and the generic results in this paper would be useful in the future in any case.

Acknowledgements

SK, KN, YO, and SCP thank the workshop, Yangpyung School 2015, for providing us an opportunity to initiate this collaboration. We are grateful for Eung Jin Chun, Satoshi Iso, Takaaki Nomura and Hiroshi Yokoya for fruitful discussions. KN thanks Koichi Hamaguchi for useful comments when the first revision had been prepared. SK was supported in part by Grant-in-Aid for Scientific Research, The Ministry of Education, Culture, Sports, Science and Technology (MEXT), No. 23104006, and Grant H2020-MSCA-RISE- 2014 No. 645722 (Non-Minimal Higgs). This work

[11] It is suggested that additional jet activity could provide a useful handle to understand the underlying physics of heavy resonance in Ref. [239].

is supported in part by NRF Research No. 2009-0083526 (YO) of the Republic of Korea. SCP is supported by the National Research Foundation of Korea (NRF) grant funded by the Korean government (MSIP) (No. 2016R1A2B2016112) and (No. 2013R1A1A2064120). This work was supported by IBS under the project code, IBS-R018-D1 for RW.

Appendix

A Brief review on the original model

Here, we briefly summarize features in the model discussed in [150].

(a) In this model, the sub-eV neutrino masses are radiatively generated at the three loop level with the loop suppression factor $1/(4\pi)^6$. In such a situation, a part of couplings, including scalar trilinear couplings, contributing to the neutrino matrix tends to be close to unity.

(b) When a scalar trilinear coupling is large, they can put a negative effect on scalar quartic couplings at the one loop level, which threatens the stability of the vacuum.

(c) The doubly charged scalar $k^{\pm\pm}$ is isolated from the charged lepton at the leading order under the assignment of the global $U(1)$ charges summarized in Tab. 1. Then, the charged particle does not contribute to lepton-flavor-violating processes significantly and a few hundred GeV mass is possible.

(d) The two singly charged scalars $h_1^\pm$ and $h_2^\pm$ have couplings to the charged leptons at the tree level. Since in our model a part of couplings are sizable, constraints from lepton flavor violations and vacuum stability do not allow a few hundred GeV masses, especially when $k^{\pm\pm}$ is around a few hundred GeV. The result of the global analysis in our previous paper [150] says that when $k^{\pm\pm}$ is 250 GeV (which is around the minimum value of $m_{k^{\pm\pm}}$), $m_{h_1^\pm}$ and $m_{h_2^\pm}$ should be greater than 3 TeV.

(e) In allowed parameter configurations, we found that the absolute value of the coupling $(y_R)_{22}$ (in front of $\bar{N}_{R_2} e^c_{R_2} h_2^-$), tends to be $8 \sim 9$, while the peak of the distribution of the scalar trilinear couplings $\mu_{11} \equiv \lambda_{11} v'/\sqrt{2}$ (in front of $h_1^- h_1^- k^{++}$) and μ_{22} (in front of $h_2^+ h_2^+ k^{--}$) is around $14 \sim 15$ TeV. We assumed that values of μ_{11} and μ_{22} are the same and real in the analysis.

(f) The two CP even components are mixed each other as shown in Eq. (2.4). By the (simplified) global analysis in [150] based on the data [230–235], the sine of the mixing angle α should be

$$|\sin\alpha| \lesssim 0.3, \tag{A.1}$$

within 2σ allowed regions.

(g) On the other hand, the observed relic density requires a specific range of $\sin\alpha$. In our model, the Majorana DM N_{R_1} communicates with the SM particles and the $U(1)$ NG boson G through the two CP even scalars h and H. When v' is $\mathcal{O}(1)$ TeV, DM$-$DM$-h/H$ couplings are significantly suppressed as (M_{N_1}/v') and then we should rely on the two scalar resonant

regions. When we consider the situation $m_{\rm DM}/2 \simeq m_h\,(\simeq 125\,{\rm GeV})$, a reasonable amount of the mixing angle α is required as

$$|\sin\alpha| \gtrsim 0.3, \tag{A.2}$$

where a tense situation with Eq. (A.1) is observed. The allowed range of v' is a function of $\sin\alpha$ and the maximum value is

$$v'|_{\rm max} \sim 9\,{\rm TeV} \text{ when } |\sin\alpha| \sim 0.3. \tag{A.3}$$

Whereas the other resonant point is selected as $m_{\rm DM}/2 \simeq m_H$, the requirement on the angle is as follows,

$$|\sin\alpha| \lesssim 0.3, \tag{A.4}$$

when $m_H = 250\,{\rm GeV}$ or a bit more. We find that the heavy H as $m_H = 500\,{\rm GeV}$ cannot explain the relic density because of the suppression in the resonant propagator of H. The maximum of v' is found as

$$v'|_{\rm max} \sim 6\,{\rm TeV} \text{ when } 0 \lesssim |\sin\alpha| \lesssim 0.05, \tag{A.5}$$

where the couplings of H to the SM particles becomes so week and hard to be excluded from the 8 TeV LHC results.

B Decay widths at one loop

Here, we summarize the forms of relevant decay widths at one-loop level in the presence of the scalar mixing in Eq. (3.23). We mention that we ignore $\Gamma_{S'\to gg}$ since this value is tiny because of the fact $\mathcal{B}(H^{\rm SM}_{750\,{\rm GeV}} \to gg) = 2.55\times10^{-2}\%$. The widths of the 125 GeV Higgs boson are used for global fits of signal strengths of the observed Higgs.

$$\Gamma_{h\to gg} = \frac{\alpha_s^2 m_h^3}{72\pi^3 v^2}\left|\frac{3}{4}\left(A^{\gamma\gamma}_{1/2}(\tau_t^{\rm SM})\right)c_\beta\right|^2, \tag{B.1}$$

$$\Gamma_{h\to\gamma\gamma} = \frac{\alpha_{\rm EM}^2 m_h^3}{256\pi^3 v^2}\left|\left(A_1^{\gamma\gamma}(\tau_W^{\rm SM}) + N_C Q_t^2 A^{\gamma\gamma}_{1/2}(\tau_t^{\rm SM})\right)c_\beta + \frac{1}{2}\frac{v[\sum_a \mu_a]}{m^2_{k^{\pm\pm}}} Q_k^2 A_0^{\gamma\gamma}(\tau_k^{\rm SM})(-s_\beta)\right|^2, \tag{B.2}$$

$$\Gamma_{h\to Z\gamma} = \frac{\alpha_{\rm EM}^2 m_h^3}{512\pi^3}\left(1-\frac{m_Z^2}{m_h^2}\right)^3\left|A^{Z\gamma}_{\rm SM}c_\beta - \frac{[\sum_a \mu_a]}{m^2_{k^{\pm\pm}}}\left(2Q_k g_{Zkk}\right)A_0^{Z\gamma}(\tau_k^{\rm SM},\lambda_k)(-s_\beta)\right|^2, \tag{B.3}$$

$$\Gamma_{S'\to\gamma\gamma} = \frac{\alpha_{\rm EM}^2 m_{S'}^3}{256\pi^3 v^2}\left|\left(A_1^{\gamma\gamma}(\tau_W) + N_C Q_t^2 A^{\gamma\gamma}_{1/2}(\tau_t)\right)s_\beta + \frac{1}{2}\frac{v[\sum_a \mu_a]}{m^2_{k^{\pm\pm}}} Q_k^2 A_0^{\gamma\gamma}(\tau_k)\,c_\beta\right|^2, \tag{B.4}$$

$$\Gamma_{S'\to Z\gamma} = \frac{\alpha_{\rm EM}^2 m_{S'}^3}{512\pi^3}\left(1-\frac{m_Z^2}{m_{S'}^2}\right)^3\left|A^{Z\gamma}_{\rm SM}(\tau^{\rm SM}_{W,t}\to\tau_{W,t})s_\beta - \frac{[\sum_a \mu_a]}{m^2_{k^{\pm\pm}}}\left(2Q_k g_{Zkk}\right)A_0^{Z\gamma}(\tau_k,\lambda_k)\,c_\beta\right|^2, \tag{B.5}$$

$$\Gamma_{S'\to ZZ} = \left|\left(\Gamma_{\rm tot}(H^{\rm SM}_{750\,{\rm GeV}})\mathcal{B}(H^{\rm SM}_{750\,{\rm GeV}}\to ZZ)\right)^{1/2} s_\beta + \mathcal{M}_{S\to ZZ}\,c_\beta\right|^2, \tag{B.6}$$

with the factors

$$A_{\rm SM}^{Z\gamma} = \frac{2}{v}\left[\cot\theta_W A_1^{Z\gamma}(\tau_W^{\rm SM},\lambda_W) + N_C\frac{(2Q_t)(T_3^{(t)}-2Q_t s_W^2)}{s_W c_W}A_{1/2}^{Z\gamma}(\tau_t^{\rm SM},\lambda_t)\right], \tag{B.7}$$

$$\mathcal{M}_{S\to ZZ} = \left\{\left(\frac{s_W^2}{2c_W^2}\right)\frac{\alpha_{\rm EM}^2 m_{S'}^3}{512\pi^3}\left(1-\frac{m_Z^2}{m_{S'}^2}\right)^3\right\}^{1/2}\left[-\frac{[\sum_a \mu_a]}{m_{k^{\pm\pm}}^2}(2Q_k g_{Zkk})\,A_0^{Z\gamma}(\tau_k,\lambda_k)\right], \tag{B.8}$$

$$A_1^{\gamma\gamma}(x) = -x^2\left[2x^{-2}+3x^{-1}+3(2x^{-1}-1)f(x^{-1})\right], \tag{B.9}$$

$$A_{1/2}^{\gamma\gamma}(x) = 2x^2\left[x^{-1}+(x^{-1}-1)f(x^{-1})\right], \tag{B.10}$$

$$A_1^{Z\gamma}(x,y) = 4(3-\tan^2\theta_W)I_2(x,y) + \left[(1+2x^{-1})\tan^2\theta_W - (5+2x^{-1})\right]I_1(x,y), \tag{B.11}$$

$$A_{1/2}^{Z\gamma}(x,y) = I_1(x,y) - I_2(x,y). \tag{B.12}$$

Here, the ratios and two functions are defined for convenience

$$\tau_i^{\rm SM} = \frac{4m_i^2}{m_h^2}, \quad \tau_i = \frac{4m_i^2}{m_{S'}^2} \quad (i=t,W,k), \tag{B.13}$$

$$I_1(x,y) = \frac{xy}{2(x-y)} + \frac{x^2y^2}{2(x-y)^2}\left[f(x^{-1})-f(y^{-1})\right] + \frac{x^2y}{(x-y)^2}\left[g(x^{-1})-g(y^{-1})\right] = A_0^{Z\gamma}(x,y), \tag{B.14}$$

$$I_2(x,y) = -\frac{xy}{2(x-y)}\left[f(x^{-1})-f(y^{-1})\right]. \tag{B.15}$$

α_s, $N_C\,(=3)$, $Q_t\,(=2/3)$ and $T_3^{(t)}\,(=1/2)$ are the fine structure constant of the QCD coupling, the QCD color factor for quarks, the electric charges of the top quark in unit of the positron's one, and the weak isospin of the top quark, respectively. Other variables were already defined around Eqs. (3.5)-(3.8). When we take the limit $s_\beta \to 0$, $\Gamma_{S'\to ZZ}$ is reduced to the form in Eq. (3.2).

C Additional plots

In this appendix, we provide plots for discussing the case that the mixing of two fields S and Φ through mass terms under the assumption $\langle S\rangle = 0$. Here, the mass parameter $m_{S'h}$ in the S'-h-h interaction is automatically determined by the two mass eigenvalues and the mixing angle β as shown in Eq. (3.26). We note that the two choices in the universal mass of doubly charged scalars (660 GeV and 900 GeV) are from the expected 95% C.L. lower bounds under the assumption $\mathcal{B}(j_a^{\pm\pm}\to\mu^\pm\mu^\pm) = 100\%$ when $N_j = 10$ and $N_j = 100$, respectively.

References

[1] **ATLAS** Collaboration, "Search for resonances decaying to photon pairs in 3.2 fb^{-1} of pp collisions at $\sqrt{s} = 13$ TeV with the ATLAS detector," Tech. Rep. ATLAS-CONF-2015-081, CERN, Geneva, Dec, 2015.

[2] **CMS** Collaboration, "Search for new physics in high mass diphoton events in proton-proton collisions at $\sqrt{s} = 13$ TeV," Tech. Rep. CMS-PAS-EXO-15-004, CERN, Geneva, 2015.

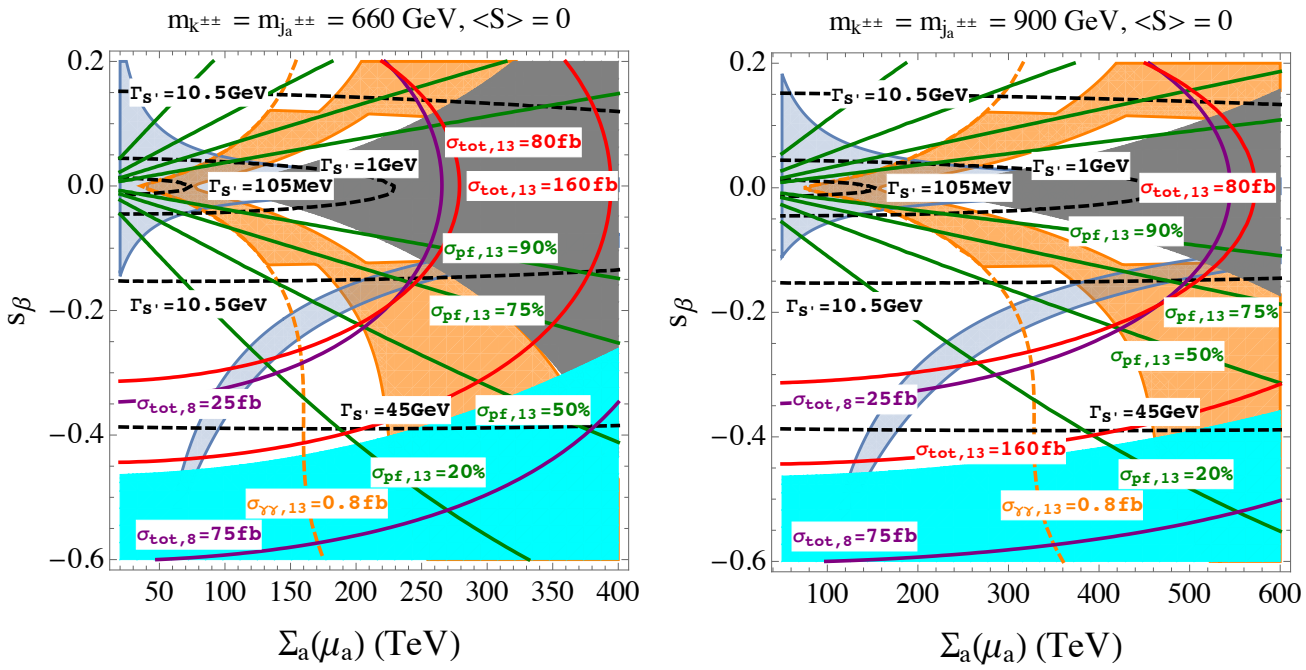

Figure 7: Allowed ranges of the parameters $\{\sum_a(\mu_a), s_\beta\}$ are shown in the two choices of the mass of the degenerated doubly charged scalars ($m_{k^{\pm\pm}}$ [$= m_{j_a^{\pm\pm}}$] $= 660/900$ GeV [left panel/right panel]). Under the assumption $\langle S\rangle = 0$, the value of $m_{S'h}$ is fixed as shown in Eq. (3.26). The light blue regions represent 2σ allowed regions of 125 GeV Higgs signal strengths, while the orange regions suggest the areas where the 750 GeV excess is suitably explained. The gray/cyan regions are excluded in 95% C.L.s by the ATLAS 8 TeV results for $S' \to \gamma\gamma/ZZ$. For better understanding, several contours for the total width of S' ($\Gamma_{S'}$), total production cross sections at $\sqrt{s} = 8/13$ TeV ($\sigma_{\rm tot,8/13}$), and the percentage of the production through the photon fusion at $\sqrt{s} = 13$ TeV ($\sigma_{\rm pf,13}$) are illustrated.

[3] **ATLAS** Collaboration, "Search for resonances in diphoton events with the ATLAS detector at $\sqrt{s} = 13$ TeV," Tech. Rep. ATLAS-CONF-2016-018, CERN, Geneva, Mar, 2016.

[4] **CMS** Collaboration, "Search for new physics in high mass diphoton events in 3.3 fb^{-1} of proton-proton collisions at $\sqrt{s} = 13$ TeV and combined interpretation of searches at 8 TeV and 13 TeV," Tech. Rep. CMS-PAS-EXO-16-018, CERN, Geneva, 2016.

[5] K. Harigaya and Y. Nomura, "Composite Models for the 750 GeV Diphoton Excess," `arXiv:1512.04850 [hep-ph]`.

[6] Y. Mambrini, G. Arcadi, and A. Djouadi, "The LHC diphoton resonance and dark matter," `arXiv:1512.04913 [hep-ph]`.

[7] M. Backovic, A. Mariotti, and D. Redigolo, "Di-photon excess illuminates Dark Matter," `arXiv:1512.04917 [hep-ph]`.

[8] A. Angelescu, A. Djouadi, and G. Moreau, "Scenarii for interpretations of the LHC diphoton excess: two Higgs doublets and vector-like quarks and leptons," `arXiv:1512.04921 [hep-ph]`.

[9] Y. Nakai, R. Sato, and K. Tobioka, "Footprints of New Strong Dynamics via Anomaly," `arXiv:1512.04924 [hep-ph]`.

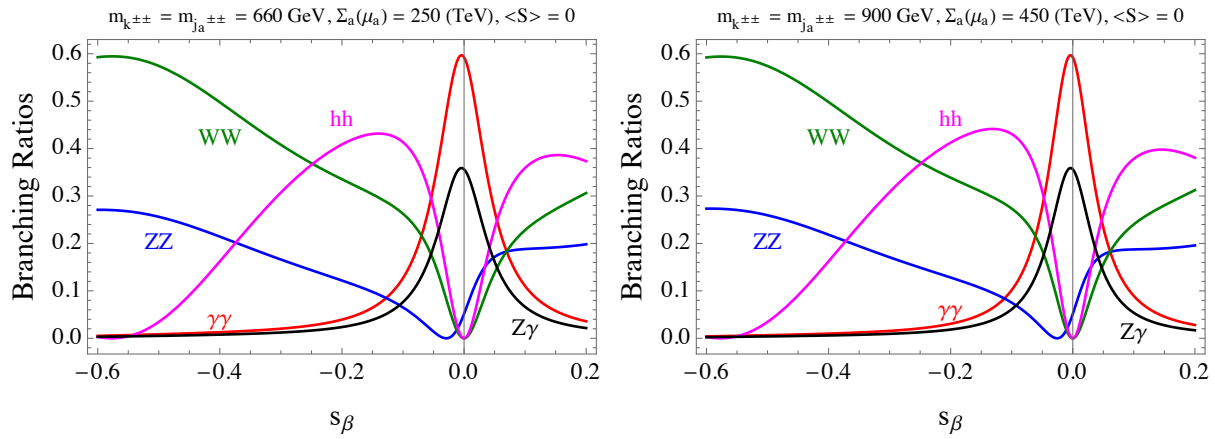

Figure 8: Relevant branching ratios of S' in the two configurations in Fig. 7 are shown. Here, values of $\Sigma_a(\mu_a)$ are suitably fixed as typical digits in the corresponding allowed regions.

[10] S. Knapen, T. Melia, M. Papucci, and K. Zurek, "Rays of light from the LHC," arXiv:1512.04928 [hep-ph].

[11] D. Buttazzo, A. Greljo, and D. Marzocca, "Knocking on New Physics' door with a Scalar Resonance," arXiv:1512.04929 [hep-ph].

[12] A. Pilaftsis, "Diphoton Signatures from Heavy Axion Decays at LHC," arXiv:1512.04931 [hep-ph].

[13] R. Franceschini, G. F. Giudice, J. F. Kamenik, M. McCullough, A. Pomarol, R. Rattazzi, M. Redi, F. Riva, A. Strumia, and R. Torre, "What is the gamma gamma resonance at 750 GeV?," arXiv:1512.04933 [hep-ph].

[14] S. Di Chiara, L. Marzola, and M. Raidal, "First interpretation of the 750 GeV di-photon resonance at the LHC," arXiv:1512.04939 [hep-ph].

[15] T. Higaki, K. S. Jeong, N. Kitajima, and F. Takahashi, "The QCD Axion from Aligned Axions and Diphoton Excess," arXiv:1512.05295 [hep-ph].

[16] S. D. McDermott, P. Meade, and H. Ramani, "Singlet Scalar Resonances and the Diphoton Excess," arXiv:1512.05326 [hep-ph].

[17] J. Ellis, S. A. R. Ellis, J. Quevillon, V. Sanz, and T. You, "On the Interpretation of a Possible $\sim$ 750 GeV Particle Decaying into $\gamma\gamma$," arXiv:1512.05327 [hep-ph].

[18] M. Low, A. Tesi, and L.-T. Wang, "A pseudoscalar decaying to photon pairs in the early LHC run 2 data," arXiv:1512.05328 [hep-ph].

[19] B. Bellazzini, R. Franceschini, F. Sala, and J. Serra, "Goldstones in Diphotons," arXiv:1512.05330 [hep-ph].

[20] R. S. Gupta, S. Jager, Y. Kats, G. Perez, and E. Stamou, "Interpreting a 750 GeV Diphoton Resonance," arXiv:1512.05332 [hep-ph].

[21] C. Petersson and R. Torre, "The 750 GeV diphoton excess from the goldstino superpartner," arXiv:1512.05333 [hep-ph].

[22] E. Molinaro, F. Sannino, and N. Vignaroli, "Strong dynamics or axion origin of the diphoton excess," arXiv:1512.05334 [hep-ph].

[23] A. Falkowski, O. Slone, and T. Volansky, "Phenomenology of a 750 GeV Singlet," arXiv:1512.05777 [hep-ph].

[24] B. Dutta, Y. Gao, T. Ghosh, I. Gogoladze, and T. Li, "Interpretation of the diphoton

excess at CMS and ATLAS," arXiv:1512.05439 [hep-ph].
[25] Q.-H. Cao, Y. Liu, K.-P. Xie, B. Yan, and D.-M. Zhang, "A Boost Test of Anomalous Diphoton Resonance at the LHC," arXiv:1512.05542 [hep-ph].
[26] S. Matsuzaki and K. Yamawaki, "750 GeV Diphoton Signal from One-Family Walking Technipion," arXiv:1512.05564 [hep-ph].
[27] A. Kobakhidze, F. Wang, L. Wu, J. M. Yang, and M. Zhang, "LHC diphoton excess explained as a heavy scalar in top-seesaw model," arXiv:1512.05585 [hep-ph].
[28] R. Martinez, F. Ochoa, and C. F. Sierra, "Diphoton decay for a 750 GeV scalar dark matter," arXiv:1512.05617 [hep-ph].
[29] P. Cox, A. D. Medina, T. S. Ray, and A. Spray, "Diphoton Excess at 750 GeV from a Radion in the Bulk-Higgs Scenario," arXiv:1512.05618 [hep-ph].
[30] D. Becirevic, E. Bertuzzo, O. Sumensari, and R. Z. Funchal, "Can the new resonance at LHC be a CP-Odd Higgs boson?," arXiv:1512.05623 [hep-ph].
[31] J. M. No, V. Sanz, and J. Setford, "See-Saw Composite Higgses at the LHC: Linking Naturalness to the 750 GeV Di-Photon Resonance," arXiv:1512.05700 [hep-ph].
[32] S. V. Demidov and D. S. Gorbunov, "On sgoldstino interpretation of the diphoton excess," arXiv:1512.05723 [hep-ph].
[33] W. Chao, R. Huo, and J.-H. Yu, "The Minimal Scalar-Stealth Top Interpretation of the Diphoton Excess," arXiv:1512.05738 [hep-ph].
[34] S. Fichet, G. von Gersdorff, and C. Royon, "Scattering Light by Light at 750 GeV at the LHC," arXiv:1512.05751 [hep-ph].
[35] D. Curtin and C. B. Verhaaren, "Quirky Explanations for the Diphoton Excess," arXiv:1512.05753 [hep-ph].
[36] L. Bian, N. Chen, D. Liu, and J. Shu, "A hidden confining world on the 750 GeV diphoton excess," arXiv:1512.05759 [hep-ph].
[37] J. Chakrabortty, A. Choudhury, P. Ghosh, S. Mondal, and T. Srivastava, "Di-photon resonance around 750 GeV: shedding light on the theory underneath," arXiv:1512.05767 [hep-ph].
[38] A. Ahmed, B. M. Dillon, B. Grzadkowski, J. F. Gunion, and Y. Jiang, "Higgs-radion interpretation of 750 GeV di-photon excess at the LHC," arXiv:1512.05771 [hep-ph].
[39] P. Agrawal, J. Fan, B. Heidenreich, M. Reece, and M. Strassler, "Experimental Considerations Motivated by the Diphoton Excess at the LHC," arXiv:1512.05775 [hep-ph].
[40] C. Csaki, J. Hubisz, and J. Terning, "The Minimal Model of a Diphoton Resonance: Production without Gluon Couplings," arXiv:1512.05776 [hep-ph].
[41] D. Aloni, K. Blum, A. Dery, A. Efrati, and Y. Nir, "On a possible large width 750 GeV diphoton resonance at ATLAS and CMS," arXiv:1512.05778 [hep-ph].
[42] Y. Bai, J. Berger, and R. Lu, "A 750 GeV Dark Pion: Cousin of a Dark G-parity-odd WIMP," arXiv:1512.05779 [hep-ph].
[43] E. Gabrielli, K. Kannike, B. Mele, M. Raidal, C. Spethmann, and H. Veermae, "A SUSY Inspired Simplified Model for the 750 GeV Diphoton Excess," arXiv:1512.05961 [hep-ph].
[44] R. Benbrik, C.-H. Chen, and T. Nomura, "Higgs singlet as a diphoton resonance in a vector-like quark model," arXiv:1512.06028 [hep-ph].
[45] J. S. Kim, J. Reuter, K. Rolbiecki, and R. R. de Austri, "A resonance without resonance: scrutinizing the diphoton excess at 750 GeV," arXiv:1512.06083 [hep-ph].

[46] A. Alves, A. G. Dias, and K. Sinha, "The 750 GeV S-cion: Where else should we look for it?," arXiv:1512.06091 [hep-ph].
[47] E. Megias, O. Pujolas, and M. Quiros, "On dilatons and the LHC diphoton excess," arXiv:1512.06106 [hep-ph].
[48] L. M. Carpenter, R. Colburn, and J. Goodman, "Supersoft SUSY Models and the 750 GeV Diphoton Excess, Beyond Effective Operators," arXiv:1512.06107 [hep-ph].
[49] J. Bernon and C. Smith, "Could the width of the diphoton anomaly signal a three-body decay ?," arXiv:1512.06113 [hep-ph].
[50] W. Chao, "Symmetries Behind the 750 GeV Diphoton Excess," arXiv:1512.06297 [hep-ph].
[51] M. T. Arun and P. Saha, "Gravitons in multiply warped scenarios - at 750 GeV and beyond," arXiv:1512.06335 [hep-ph].
[52] C. Han, H. M. Lee, M. Park, and V. Sanz, "The diphoton resonance as a gravity mediator of dark matter," arXiv:1512.06376 [hep-ph].
[53] S. Chang, "A Simple $U(1)$ Gauge Theory Explanation of the Diphoton Excess," arXiv:1512.06426 [hep-ph].
[54] I. Chakraborty and A. Kundu, "Diphoton excess at 750 GeV: Singlet scalars confront naturalness," arXiv:1512.06508 [hep-ph].
[55] R. Ding, L. Huang, T. Li, and B. Zhu, "Interpreting 750 GeV Diphoton Excess with R-parity Violation Supersymmetry," arXiv:1512.06560 [hep-ph].
[56] H. Han, S. Wang, and S. Zheng, "Scalar Dark Matter Explanation of Diphoton Excess at LHC," arXiv:1512.06562 [hep-ph].
[57] X.-F. Han and L. Wang, "Implication of the 750 GeV diphoton resonance on two-Higgs-doublet model and its extensions with Higgs field," arXiv:1512.06587 [hep-ph].
[58] M.-x. Luo, K. Wang, T. Xu, L. Zhang, and G. Zhu, "Squarkonium/Diquarkonium and the Di-photon Excess," arXiv:1512.06670 [hep-ph].
[59] J. Chang, K. Cheung, and C.-T. Lu, "Interpreting the 750 GeV Di-photon Resonance using photon-jets in Hidden-Valley-like models," arXiv:1512.06671 [hep-ph].
[60] D. Bardhan, D. Bhatia, A. Chakraborty, U. Maitra, S. Raychaudhuri, and T. Samui, "Radion Candidate for the LHC Diphoton Resonance," arXiv:1512.06674 [hep-ph].
[61] T.-F. Feng, X.-Q. Li, H.-B. Zhang, and S.-M. Zhao, "The LHC 750 GeV diphoton excess in supersymmetry with gauged baryon and lepton numbers," arXiv:1512.06696 [hep-ph].
[62] O. Antipin, M. Mojaza, and F. Sannino, "A natural Coleman-Weinberg theory explains the diphoton excess," arXiv:1512.06708 [hep-ph].
[63] F. Wang, L. Wu, J. M. Yang, and M. Zhang, "750 GeV Diphoton Resonance, 125 GeV Higgs and Muon g-2 Anomaly in Deflected Anomaly Mediation SUSY Breaking Scenario," arXiv:1512.06715 [hep-ph].
[64] J. Cao, C. Han, L. Shang, W. Su, J. M. Yang, and Y. Zhang, "Interpreting the 750 GeV diphoton excess by the singlet extension of the Manohar-Wise Model," arXiv:1512.06728 [hep-ph].
[65] F. P. Huang, C. S. Li, Z. L. Liu, and Y. Wang, "750 GeV Diphoton Excess from Cascade Decay," arXiv:1512.06732 [hep-ph].
[66] W. Liao and H.-q. Zheng, "Scalar resonance at 750 GeV as composite of heavy vector-like fermions," arXiv:1512.06741 [hep-ph].
[67] J. J. Heckman, "750 GeV Diphotons from a D3-brane," arXiv:1512.06773 [hep-ph].

[68] M. Dhuria and G. Goswami, "Perturbativity, vacuum stability and inflation in the light of 750 GeV diphoton excess," arXiv:1512.06782 [hep-ph].
[69] X.-J. Bi, Q.-F. Xiang, P.-F. Yin, and Z.-H. Yu, "The 750 GeV diphoton excess at the LHC and dark matter constraints," arXiv:1512.06787 [hep-ph].
[70] J. S. Kim, K. Rolbiecki, and R. R. de Austri, "Model-independent combination of diphoton constraints at 750 GeV," arXiv:1512.06797 [hep-ph].
[71] L. Berthier, J. M. Cline, W. Shepherd, and M. Trott, "Effective interpretations of a diphoton excess," arXiv:1512.06799 [hep-ph].
[72] W. S. Cho, D. Kim, K. Kong, S. H. Lim, K. T. Matchev, J.-C. Park, and M. Park, "The 750 GeV Diphoton Excess May Not Imply a 750 GeV Resonance," arXiv:1512.06824 [hep-ph].
[73] J. M. Cline and Z. Liu, "LHC diphotons from electroweakly pair-produced composite pseudoscalars," arXiv:1512.06827 [hep-ph].
[74] M. Bauer and M. Neubert, "Flavor Anomalies, the Diphoton Excess and a Dark Matter Candidate," arXiv:1512.06828 [hep-ph].
[75] M. Chala, M. Duerr, F. Kahlhoefer, and K. Schmidt-Hoberg, "Tricking Landau-Yang: How to obtain the diphoton excess from a vector resonance," arXiv:1512.06833 [hep-ph].
[76] D. Barducci, A. Goudelis, S. Kulkarni, and D. Sengupta, "One jet to rule them all: monojet constraints and invisible decays of a 750 GeV diphoton resonance," arXiv:1512.06842 [hep-ph].
[77] G. M. Pelaggi, A. Strumia, and E. Vigiani, "Trinification can explain the di-photon and di-boson LHC anomalies," arXiv:1512.07225 [hep-ph].
[78] S. M. Boucenna, S. Morisi, and A. Vicente, "The LHC diphoton resonance from gauge symmetry," arXiv:1512.06878 [hep-ph].
[79] C. W. Murphy, "Vector Leptoquarks and the 750 GeV Diphoton Resonance at the LHC," arXiv:1512.06976 [hep-ph].
[80] A. E. C. Hernández and I. Nisandzic, "LHC diphoton 750 GeV resonance as an indication of $SU(3)_c \times SU(3)_L \times U(1)_X$ gauge symmetry," arXiv:1512.07165 [hep-ph].
[81] U. K. Dey, S. Mohanty, and G. Tomar, "750 GeV resonance in the Dark Left-Right Model," arXiv:1512.07212 [hep-ph].
[82] J. de Blas, J. Santiago, and R. Vega-Morales, "New vector bosons and the diphoton excess," arXiv:1512.07229 [hep-ph].
[83] A. Belyaev, G. Cacciapaglia, H. Cai, T. Flacke, A. Parolini, and H. Serôdio, "Singlets in Composite Higgs Models in light of the LHC di-photon searches," arXiv:1512.07242 [hep-ph].
[84] P. S. B. Dev and D. Teresi, "Asymmetric Dark Matter in the Sun and the Diphoton Excess at the LHC," arXiv:1512.07243 [hep-ph].
[85] W.-C. Huang, Y.-L. S. Tsai, and T.-C. Yuan, "Gauged Two Higgs Doublet Model confronts the LHC 750 GeV di-photon anomaly," arXiv:1512.07268 [hep-ph].
[86] S. Moretti and K. Yagyu, "The 750 GeV diphoton excess and its explanation in 2-Higgs Doublet Models with a real inert scalar multiplet," arXiv:1512.07462 [hep-ph].
[87] K. M. Patel and P. Sharma, "Interpreting 750 GeV diphoton excess in SU(5) grand unified theory," arXiv:1512.07468 [hep-ph].
[88] M. Badziak, "Interpreting the 750 GeV diphoton excess in minimal extensions of Two-Higgs-Doublet models," arXiv:1512.07497 [hep-ph].
[89] S. Chakraborty, A. Chakraborty, and S. Raychaudhuri, "Diphoton resonance at 750 GeV in the broken MRSSM," arXiv:1512.07527 [hep-ph].

[90] Q.-H. Cao, S.-L. Chen, and P.-H. Gu, "Strong CP Problem, Neutrino Masses and the 750 GeV Diphoton Resonance," arXiv:1512.07541 [hep-ph].
[91] W. Altmannshofer, J. Galloway, S. Gori, A. L. Kagan, A. Martin, and J. Zupan, "On the 750 GeV di-photon excess," arXiv:1512.07616 [hep-ph].
[92] M. Cvetič, J. Halverson, and P. Langacker, "String Consistency, Heavy Exotics, and the 750 GeV Diphoton Excess at the LHC," arXiv:1512.07622 [hep-ph].
[93] J. Gu and Z. Liu, "Running after Diphoton," arXiv:1512.07624 [hep-ph].
[94] B. C. Allanach, P. S. B. Dev, S. A. Renner, and K. Sakurai, "Di-photon Excess Explained by a Resonant Sneutrino in R-parity Violating Supersymmetry," arXiv:1512.07645 [hep-ph].
[95] H. Davoudiasl and C. Zhang, "A 750 GeV Messenger of Dark Conformal Symmetry Breaking," arXiv:1512.07672 [hep-ph].
[96] N. Craig, P. Draper, C. Kilic, and S. Thomas, "How the $\gamma\gamma$ Resonance Stole Christmas," arXiv:1512.07733 [hep-ph].
[97] K. Das and S. K. Rai, "The 750 GeV Diphoton excess in a $U(1)$ hidden symmetry model," arXiv:1512.07789 [hep-ph].
[98] K. Cheung, P. Ko, J. S. Lee, J. Park, and P.-Y. Tseng, "A Higgcision study on the 750 GeV Di-photon Resonance and 125 GeV SM Higgs boson with the Higgs-Singlet Mixing," arXiv:1512.07853 [hep-ph].
[99] J. Liu, X.-P. Wang, and W. Xue, "LHC diphoton excess from colorful resonances," arXiv:1512.07885 [hep-ph].
[100] J. Zhang and S. Zhou, "Electroweak Vacuum Stability and Diphoton Excess at 750 GeV," arXiv:1512.07889 [hep-ph].
[101] J. A. Casas, J. R. Espinosa, and J. M. Moreno, "The 750 GeV Diphoton Excess as a First Light on Supersymmetry Breaking," arXiv:1512.07895 [hep-ph].
[102] L. J. Hall, K. Harigaya, and Y. Nomura, "750 GeV Diphotons: Implications for Supersymmetric Unification," arXiv:1512.07904 [hep-ph].
[103] H. Han, S. Wang, and S. Zheng, "Dark Matter Theories in the Light of Diphoton Excess," arXiv:1512.07992 [hep-ph].
[104] J.-C. Park and S. C. Park, "Indirect signature of dark matter with the diphoton resonance at 750 GeV," arXiv:1512.08117 [hep-ph].
[105] A. Salvio and A. Mazumdar, "Higgs Stability and the 750 GeV Diphoton Excess," arXiv:1512.08184 [hep-ph].
[106] D. Chway, R. Dermíšek, T. H. Jung, and H. D. Kim, "Glue to light signal of a new particle," arXiv:1512.08221 [hep-ph].
[107] G. Li, Y.-n. Mao, Y.-L. Tang, C. Zhang, Y. Zhou, and S.-h. Zhu, "A Loop-philic Pseudoscalar," arXiv:1512.08255 [hep-ph].
[108] M. Son and A. Urbano, "A new scalar resonance at 750 GeV: Towards a proof of concept in favor of strongly interacting theories," arXiv:1512.08307 [hep-ph].
[109] Y.-L. Tang and S.-h. Zhu, "NMSSM extended with vector-like particles and the diphoton excess on the LHC," arXiv:1512.08323 [hep-ph].
[110] H. An, C. Cheung, and Y. Zhang, "Broad Diphotons from Narrow States," arXiv:1512.08378 [hep-ph].
[111] J. Cao, F. Wang, and Y. Zhang, "Interpreting The 750 GeV Diphton Excess Within TopFlavor Seesaw Model," arXiv:1512.08392 [hep-ph].
[112] F. Wang, W. Wang, L. Wu, J. M. Yang, and M. Zhang, "Interpreting 750 GeV Diphoton

Resonance in the NMSSM with Vector-like Particles," arXiv:1512.08434 [hep-ph].
[113] C. Cai, Z.-H. Yu, and H.-H. Zhang, "The 750 GeV diphoton resonance as a singlet scalar in an extra dimensional model," arXiv:1512.08440 [hep-ph].
[114] Q.-H. Cao, Y. Liu, K.-P. Xie, B. Yan, and D.-M. Zhang, "The Diphoton Excess, Low Energy Theorem and the 331 Model," arXiv:1512.08441 [hep-ph].
[115] J. E. Kim, "Is an axizilla possible for di-photon resonance?," arXiv:1512.08467 [hep-ph].
[116] J. Gao, H. Zhang, and H. X. Zhu, "Diphoton excess at 750 GeV: gluon-gluon fusion or quark-antiquark annihilation?," arXiv:1512.08478 [hep-ph].
[117] W. Chao, "Neutrino Catalyzed Diphoton Excess," arXiv:1512.08484 [hep-ph].
[118] X.-J. Bi, R. Ding, Y. Fan, L. Huang, C. Li, T. Li, S. Raza, X.-C. Wang, and B. Zhu, "A Promising Interpretation of Diphoton Resonance at 750 GeV," arXiv:1512.08497 [hep-ph].
[119] F. Goertz, J. F. Kamenik, A. Katz, and M. Nardecchia, "Indirect Constraints on the Scalar Di-Photon Resonance at the LHC," arXiv:1512.08500 [hep-ph].
[120] L. A. Anchordoqui, I. Antoniadis, H. Goldberg, X. Huang, D. Lust, and T. R. Taylor, "750 GeV diphotons from closed string states," arXiv:1512.08502 [hep-ph].
[121] P. S. B. Dev, R. N. Mohapatra, and Y. Zhang, "Quark Seesaw Vectorlike Fermions and Diphoton Excess," arXiv:1512.08507 [hep-ph].
[122] N. Bizot, S. Davidson, M. Frigerio, and J. L. Kneur, "Two Higgs doublets to explain the excesses $pp \to \gamma\gamma(750\text{ GeV})$ and $h \to \tau^{\pm}\mu^{\mp}$," arXiv:1512.08508 [hep-ph].
[123] Y. Hamada, T. Noumi, S. Sun, and G. Shiu, "An O(750) GeV Resonance and Inflation," arXiv:1512.08984 [hep-ph].
[124] S. Kanemura, N. Machida, S. Odori, and T. Shindou, "Diphoton excess at 750 GeV in an extended scalar sector," arXiv:1512.09053 [hep-ph].
[125] Y. Jiang, Y.-Y. Li, and T. Liu, "750 GeV Resonance in the Gauged $U(1)'$-Extended MSSM," arXiv:1512.09127 [hep-ph].
[126] **ATLAS** Collaboration, G. Aad *et al.*, "Search for high-mass diphoton resonances in pp collisions at $\sqrt{s} = 8$ TeV with the ATLAS detector," *Phys. Rev.* **D92** no. 3, (2015) 032004, arXiv:1504.05511 [hep-ex].
[127] **CMS** Collaboration, "Search for new resonances in the diphoton final state in the range between 150 and 850 GeV in pp collisions at $\sqrt{s} = 8$ TeV," Tech. Rep. CMS-PAS-HIG-14-006, CERN, Geneva, 2014.
[128] "https://twiki.cern.ch/twiki/bin/view/lhcphysics/cernyellowreportpageat1314tev.".
[129] **LHC Higgs Cross Section Working Group** Collaboration, J. R. Andersen *et al.*, "Handbook of LHC Higgs Cross Sections: 3. Higgs Properties," arXiv:1307.1347 [hep-ph].
[130] **ATLAS** Collaboration, G. Aad *et al.*, "Search for an additional, heavy Higgs boson in the $H \to ZZ$ decay channel at $\sqrt{s} = 8$ TeV in pp collision data with the ATLAS detector," *Eur. Phys. J.* **C76** no. 1, (2016) 45, arXiv:1507.05930 [hep-ex].
[131] A. Zee, "A Theory of Lepton Number Violation, Neutrino Majorana Mass, and Oscillation," *Phys. Lett.* **B93** (1980) 389. [Erratum: Phys. Lett.B95,461(1980)].
[132] T. P. Cheng and L.-F. Li, "Neutrino Masses, Mixings and Oscillations in SU(2) x U(1) Models of Electroweak Interactions," *Phys. Rev.* **D22** (1980) 2860.
[133] A. Zee, "Quantum Numbers of Majorana Neutrino Masses," *Nucl. Phys.* **B264** (1986) 99.
[134] K. S. Babu, "Model of 'Calculable' Majorana Neutrino Masses," *Phys. Lett.* **B203** (1988) 132.

[135] E. Ma, "Verifiable radiative seesaw mechanism of neutrino mass and dark matter," *Phys. Rev.* **D73** (2006) 077301, arXiv:hep-ph/0601225 [hep-ph].
[136] L. M. Krauss, S. Nasri, and M. Trodden, "A Model for neutrino masses and dark matter," *Phys. Rev.* **D67** (2003) 085002, arXiv:hep-ph/0210389 [hep-ph].
[137] M. Aoki, S. Kanemura, and O. Seto, "Neutrino mass, Dark Matter and Baryon Asymmetry via TeV-Scale Physics without Fine-Tuning," *Phys. Rev. Lett.* **102** (2009) 051805, arXiv:0807.0361 [hep-ph].
[138] M. Aoki, S. Kanemura, and K. Yagyu, "Triviality and vacuum stability bounds in the three-loop neutrino mass model," *Phys. Rev.* **D83** (2011) 075016, arXiv:1102.3412 [hep-ph].
[139] M. Gustafsson, J. M. No, and M. A. Rivera, "Predictive Model for Radiatively Induced Neutrino Masses and Mixings with Dark Matter," *Phys. Rev. Lett.* **110** no. 21, (2013) 211802, arXiv:1212.4806 [hep-ph]. [Erratum: Phys. Rev. Lett.112,no.25,259902(2014)].
[140] Y. Kajiyama, H. Okada, and K. Yagyu, "T_7 Flavor Model in Three Loop Seesaw and Higgs Phenomenology," *JHEP* **10** (2013) 196, arXiv:1307.0480 [hep-ph].
[141] A. Ahriche, C.-S. Chen, K. L. McDonald, and S. Nasri, "Three-loop model of neutrino mass with dark matter," *Phys. Rev.* **D90** (2014) 015024, arXiv:1404.2696 [hep-ph].
[142] A. Ahriche, K. L. McDonald, and S. Nasri, "A Model of Radiative Neutrino Mass: with or without Dark Matter," *JHEP* **10** (2014) 167, arXiv:1404.5917 [hep-ph].
[143] C.-S. Chen, K. L. McDonald, and S. Nasri, "A Class of Three-Loop Models with Neutrino Mass and Dark Matter," *Phys. Lett.* **B734** (2014) 388–393, arXiv:1404.6033 [hep-ph].
[144] H. Okada and Y. Orikasa, "X-ray line in Radiative Neutrino Model with Global $U(1)$ Symmetry," *Phys. Rev.* **D90** no. 7, (2014) 075023, arXiv:1407.2543 [hep-ph].
[145] H. Hatanaka, K. Nishiwaki, H. Okada, and Y. Orikasa, "A Three-Loop Neutrino Model with Global $U(1)$ Symmetry," *Nucl. Phys.* **B894** (2015) 268–283, arXiv:1412.8664 [hep-ph].
[146] L.-G. Jin, R. Tang, and F. Zhang, "A three-loop radiative neutrino mass model with dark matter," *Phys. Lett.* **B741** (2015) 163–167, arXiv:1501.02020 [hep-ph].
[147] P. Culjak, K. Kumericki, and I. Picek, "Scotogenic RνMDM at three-loop level," *Phys. Lett.* **B744** (2015) 237–243, arXiv:1502.07887 [hep-ph].
[148] C.-Q. Geng, D. Huang, and L.-H. Tsai, "Comment on "A three-loop radiative neutrino mass model with dark matter" [Phys. Lett. B 741 (2015) 163]," *Phys. Lett.* **B745** (2015) 56–57, arXiv:1504.05468 [hep-ph].
[149] A. Ahriche, K. L. McDonald, S. Nasri, and T. Toma, "A Model of Neutrino Mass and Dark Matter with an Accidental Symmetry," *Phys. Lett.* **B746** (2015) 430–435, arXiv:1504.05755 [hep-ph].
[150] K. Nishiwaki, H. Okada, and Y. Orikasa, "Three loop neutrino model with isolated $k^{\pm\pm}$," *Phys. Rev.* **D92** no. 9, (2015) 093013, arXiv:1507.02412 [hep-ph].
[151] H. Okada and K. Yagyu, "Three-loop Neutrino Mass Model with Doubly Charged Particles from Iso-Doublets," arXiv:1508.01046 [hep-ph].
[152] A. Ahriche, K. L. McDonald, and S. Nasri, "A Radiative Model for the Weak Scale and Neutrino Mass via Dark Matter," arXiv:1508.02607 [hep-ph].
[153] A. Ahriche, K. L. McDonald, and S. Nasri, "Scalar Sector Phenomenology of Three-Loop Radiative Neutrino Mass Models," *Phys. Rev.* **D92** no. 9, (2015) 095020, arXiv:1508.05881 [hep-ph].
[154] T. Nomura and H. Okada, "Four-loop Neutrino Model Inspired by Diphoton Excess at 750 GeV," *Phys. Lett.* **B755** (2016) 306–311, arXiv:1601.00386 [hep-ph].

[155] T. Nomura and H. Okada, "Four-loop Radiative Seesaw Model with 750 GeV Diphoton Resonance," arXiv:1601.04516 [hep-ph].
[156] H. Okada and K. Yagyu, "Renormalizable model for neutrino mass, dark matter, muon $g-2$ and 750 GeV diphoton excess," *Phys. Lett.* **B756** (2016) 337–344, arXiv:1601.05038 [hep-ph].
[157] T. Nomura and H. Okada, "Generalized Zee-Babu model with 750 GeV diphoton resonance," *Phys. Lett.* **B756** (2016) 295–302, arXiv:1601.07339 [hep-ph].
[158] C. Arbeláez, A. E. C. Hernández, S. Kovalenko, and I. Schmidt, "Linking radiative seesaw-type mechanism of fermion masses and non-trivial quark mixing with the 750 GeV diphoton excess," arXiv:1602.03607 [hep-ph].
[159] P. Ko, T. Nomura, H. Okada, and Y. Orikasa, "Confronting a New Three-loop Seesaw Model with the 750 GeV Diphoton Excess," arXiv:1602.07214 [hep-ph].
[160] S. C. Park and J. Shu, "Split Universal Extra Dimensions and Dark Matter," *Phys. Rev.* **D79** (2009) 091702, arXiv:0901.0720 [hep-ph].
[161] C.-R. Chen, M. M. Nojiri, S. C. Park, J. Shu, and M. Takeuchi, "Dark matter and collider phenomenology of split-UED," *JHEP* **09** (2009) 078, arXiv:0903.1971 [hep-ph].
[162] C.-R. Chen, M. M. Nojiri, S. C. Park, and J. Shu, "Kaluza-Klein Dark Matter After Fermi," arXiv:0908.4317 [hep-ph].
[163] S. C. Park and J. Shu, "Dark Matter and Collider Physics in Split-UED," *AIP Conf. Proc.* **1200** (2010) 587–590, arXiv:0910.0931 [hep-ph]. [AIP Conf. Proc.1200,1051(2010)].
[164] K. Kong, S. C. Park, and T. G. Rizzo, "Collider Phenomenology with Split-UED," *JHEP* **04** (2010) 081, arXiv:1002.0602 [hep-ph].
[165] K. Kong, S. C. Park, and T. G. Rizzo, "A vector-like fourth generation with a discrete symmetry from Split-UED," *JHEP* **07** (2010) 059, arXiv:1004.4635 [hep-ph].
[166] C. Csaki, J. Heinonen, J. Hubisz, S. C. Park, and J. Shu, "5D UED: Flat and Flavorless," *JHEP* **01** (2011) 089, arXiv:1007.0025 [hep-ph].
[167] K. Nishiwaki, "Higgs production and decay processes via loop diagrams in various 6D Universal Extra Dimension Models at LHC," *JHEP* **05** (2012) 111, arXiv:1101.0649 [hep-ph].
[168] K. Nishiwaki, K.-y. Oda, N. Okuda, and R. Watanabe, "A Bound on Universal Extra Dimension Models from up to $2\,\mathrm{fb}^{-1}$ of LHC Data at 7TeV," *Phys. Lett.* **B707** (2012) 506–511, arXiv:1108.1764 [hep-ph].
[169] K. Nishiwaki, K.-y. Oda, N. Okuda, and R. Watanabe, "Heavy Higgs at Tevatron and LHC in Universal Extra Dimension Models," *Phys. Rev.* **D85** (2012) 035026, arXiv:1108.1765 [hep-ph].
[170] D. Kim, Y. Oh, and S. C. Park, "W' at the LHC with $\sqrt{s} = 14\,\mathrm{TeV}$: Split universal extra dimension model," *J. Korean Phys. Soc.* **67** (2015) 1137–1141, arXiv:1109.1870 [hep-ph].
[171] A. Datta, K. Nishiwaki, and S. Niyogi, "Non-minimal Universal Extra Dimensions: The Strongly Interacting Sector at the Large Hadron Collider," *JHEP* **11** (2012) 154, arXiv:1206.3987 [hep-ph].
[172] T. Flacke, K. Kong, and S. C. Park, "Phenomenology of Universal Extra Dimensions with Bulk-Masses and Brane-Localized Terms," *JHEP* **05** (2013) 111, arXiv:1303.0872 [hep-ph].
[173] T. Kakuda, K. Nishiwaki, K.-y. Oda, and R. Watanabe, "Universal extra dimensions after Higgs discovery," *Phys. Rev.* **D88** (2013) 035007, arXiv:1305.1686 [hep-ph].
[174] T. Flacke, K. Kong, and S. C. Park, "126 GeV Higgs in Next-to-Minimal Universal Extra

Dimensions," *Phys. Lett.* **B728** (2014) 262–267, arXiv:1309.7077 [hep-ph].
[175] A. Datta, K. Nishiwaki, and S. Niyogi, "Non-minimal Universal Extra Dimensions with Brane Local Terms: The Top Quark Sector," *JHEP* **01** (2014) 104, arXiv:1310.6994 [hep-ph].
[176] H. Dohi, T. Kakuda, K. Nishiwaki, K.-y. Oda, and N. Okuda, "Notes on sphere-based universal extra dimensions," *Afr. Rev. Phys.* **9** (2014) 0069, arXiv:1406.1954 [hep-ph].
[177] T. Flacke, K. Kong, and S. C. Park, "A Review on Non-Minimal Universal Extra Dimensions," *Mod. Phys. Lett.* **A30** no. 05, (2015) 1530003, arXiv:1408.4024 [hep-ph].
[178] H. M. Lee, D. Kim, K. Kong, and S. C. Park, "Diboson Excesses Demystified in Effective Field Theory Approach," *JHEP* **11** (2015) 150, arXiv:1507.06312 [hep-ph].
[179] J. R. Ellis, M. K. Gaillard, and D. V. Nanopoulos, "A Phenomenological Profile of the Higgs Boson," *Nucl. Phys.* **B106** (1976) 292.
[180] M. A. Shifman, A. I. Vainshtein, M. B. Voloshin, and V. I. Zakharov, "Low-Energy Theorems for Higgs Boson Couplings to Photons," *Sov. J. Nucl. Phys.* **30** (1979) 711–716. [Yad. Fiz.30,1368(1979)].
[181] A. Djouadi, "The Anatomy of electro-weak symmetry breaking. I: The Higgs boson in the standard model," *Phys. Rept.* **457** (2008) 1–216, arXiv:hep-ph/0503172 [hep-ph].
[182] M. Carena, I. Low, and C. E. M. Wagner, "Implications of a Modified Higgs to Diphoton Decay Width," *JHEP* **08** (2012) 060, arXiv:1206.1082 [hep-ph].
[183] C.-S. Chen, C.-Q. Geng, D. Huang, and L.-H. Tsai, "New Scalar Contributions to $h \to Z\gamma$," *Phys. Rev.* **D87** (2013) 075019, arXiv:1301.4694 [hep-ph].
[184] L. A. Harland-Lang, V. A. Khoze, and M. G. Ryskin, "The production of a diphoton resonance via photon-photon fusion," *JHEP* **03** (2016) 182, arXiv:1601.07187 [hep-ph].
[185] A. D. Martin and M. G. Ryskin, "The photon PDF of the proton," *Eur. Phys. J.* **C74** (2014) 3040, arXiv:1406.2118 [hep-ph].
[186] U. Danielsson, R. Enberg, G. Ingelman, and T. Mandal, "The force awakens - the 750 GeV diphoton excess at the LHC from a varying electromagnetic coupling," arXiv:1601.00624 [hep-ph].
[187] C. Csaki, J. Hubisz, S. Lombardo, and J. Terning, "Gluon vs. Photon Production of a 750 GeV Diphoton Resonance," arXiv:1601.00638 [hep-ph].
[188] H. Ito, T. Moroi, and Y. Takaesu, "Studying 750 GeV di-photon resonance at photonphoton collider," *Phys. Lett.* **B756** (2016) 147–152, arXiv:1601.01144 [hep-ph].
[189] F. D'Eramo, J. de Vries, and P. Panci, "A 750 GeV Portal: LHC Phenomenology and Dark Matter Candidates," arXiv:1601.01571 [hep-ph].
[190] I. Sahin, "Semi-elastic cross section for a scalar resonance of mass 750 GeV," arXiv:1601.01676 [hep-ph].
[191] S. Fichet, G. von Gersdorff, and C. Royon, "Measuring the diphoton coupling of a 750 GeV resonance," arXiv:1601.01712 [hep-ph].
[192] L. A. Harland-Lang, V. A. Khoze, and M. G. Ryskin, "The photon PDF in events with rapidity gaps," arXiv:1601.03772 [hep-ph].
[193] D. B. Franzosi and M. T. Frandsen, "Symmetries and composite dynamics for the 750 GeV diphoton excess," arXiv:1601.05357 [hep-ph].
[194] S. Abel and V. V. Khoze, "Photo-production of a 750 GeV di-photon resonance mediated by Kaluza-Klein leptons in the loop," arXiv:1601.07167 [hep-ph].
[195] I. Ben-Dayan and R. Brustein, "Hypercharge Axion and the Diphoton 750 GeV Resonance," arXiv:1601.07564 [hep-ph].

[196] A. D. Martin and M. G. Ryskin, "Advantages of exclusive production to probe high mass systems," *J. Phys.* **G43** no. 4, (2016) 04LT02, arXiv:1601.07774 [hep-ph].
[197] N. D. Barrie, A. Kobakhidze, M. Talia, and L. Wu, "750 GeV Composite Axion as the LHC Diphoton Resonance," *Phys. Lett.* **B755** (2016) 343–347, arXiv:1602.00475 [hep-ph].
[198] H. Ito, T. Moroi, and Y. Takaesu, "Di-Higgs Decay of Stoponium at Future Photon-Photon Collider," arXiv:1602.01231 [hep-ph].
[199] C. Gross, O. Lebedev, and J. M. No, "Drell-Yan Constraints on New Electroweak States and the Di-photon Anomaly," arXiv:1602.03877 [hep-ph].
[200] S. Baek and J.-h. Park, "LHC 750 GeV diphoton excess and muon $(g-2)$," arXiv:1602.05588 [hep-ph].
[201] E. Molinaro, F. Sannino, and N. Vignaroli, "Collider Tests of (Composite) Diphoton Resonances," arXiv:1602.07574 [hep-ph].
[202] G. Panico, L. Vecchi, and A. Wulzer, "Resonant Diphoton Phenomenology Simplified," arXiv:1603.04248 [hep-ph].
[203] A. Bharucha, A. Djouadi, and A. Goudelis, "Threshold enhancement of diphoton resonances," arXiv:1603.04464 [hep-ph].
[204] M. Ababekri, S. Dulat, J. Isaacson, C. Schmidt, and C. P. Yuan, "Implication of CMS data on photon PDFs," arXiv:1603.04874 [hep-ph].
[205] L. A. Anchordoqui, I. Antoniadis, H. Goldberg, X. Huang, D. Lust, and T. R. Taylor, "Update on 750 GeV diphotons from closed string states," arXiv:1603.08294 [hep-ph].
[206] K. Howe, S. Knapen, and D. J. Robinson, "Diphotons from an Electroweak Triplet-Singlet," arXiv:1603.08932 [hep-ph].
[207] M. T. Frandsen and I. M. Shoemaker, "Asymmetric Dark Matter Models and the LHC Diphoton Excess," arXiv:1603.09354 [hep-ph].
[208] C. F. von Weizsacker, "Radiation emitted in collisions of very fast electrons," *Z. Phys.* **88** (1934) 612–625.
[209] E. J. Williams, "Nature of the high-energy particles of penetrating radiation and status of ionization and radiation formulae," *Phys. Rev.* **45** (1934) 729–730.
[210] **ATLAS** Collaboration, G. Aad *et al.*, "Search for new resonances in $W\gamma$ and $Z\gamma$ final states in pp collisions at $\sqrt{s} = 8$ TeV with the ATLAS detector," *Phys. Lett.* **B738** (2014) 428–447, arXiv:1407.8150 [hep-ex].
[211] "Search for heavy resonances decaying to a Z boson and a photon in pp collisions at $\sqrt{s} = 13$ TeV with the ATLAS detector," Tech. Rep. ATLAS-CONF-2016-010, CERN, Geneva, Mar, 2016.
[212] "Search for ZZ resonances in the $\ell\ell qq$ final state in pp collisions at $\sqrt{s} = 13$ TeV with the ATLAS detector," Tech. Rep. ATLAS-CONF-2016-016, CERN, Geneva, Mar, 2016.
[213] **ATLAS** Collaboration, G. Aad *et al.*, "Search for a high-mass Higgs boson decaying to a W boson pair in pp collisions at $\sqrt{s} = 8$ TeV with the ATLAS detector," *JHEP* **01** (2016) 032, arXiv:1509.00389 [hep-ex].
[214] "A search for resonant Higgs-pair production in the $b\bar{b}b\bar{b}$ final state in pp collisions at $\sqrt{s} = 8$ TeV," Tech. Rep. ATLAS-CONF-2014-005, CERN, Geneva, Mar, 2014.
[215] J. F. Kamenik, B. R. Safdi, Y. Soreq, and J. Zupan, "Comments on the diphoton excess: critical reappraisal of effective field theory interpretations," arXiv:1603.06566 [hep-ph].
[216] A. Schuessler and D. Zeppenfeld, "Unitarity constraints on MSSM trilinear couplings," in *SUSY 2007 proceedings, 15th International Conference on Supersymmetry and Unification of Fundamental Interactions, July 26 - August 1, 2007, Karlsruhe, Germany*. 2007. arXiv:0710.5175 [hep-ph].

[217] **ATLAS** Collaboration, G. Aad *et al.*, "Search for anomalous production of prompt same-sign lepton pairs and pair-produced doubly charged Higgs bosons with $\sqrt{s} = 8$ TeV pp collisions using the ATLAS detector," *JHEP* **03** (2015) 041, arXiv:1412.0237 [hep-ex].

[218] J. Alwall, M. Herquet, F. Maltoni, O. Mattelaer, and T. Stelzer, "MadGraph 5 : Going Beyond," *JHEP* **06** (2011) 128, arXiv:1106.0522 [hep-ph].

[219] J. Alwall, R. Frederix, S. Frixione, V. Hirschi, F. Maltoni, O. Mattelaer, H. S. Shao, T. Stelzer, P. Torrielli, and M. Zaro, "The automated computation of tree-level and next-to-leading order differential cross sections, and their matching to parton shower simulations," *JHEP* **07** (2014) 079, arXiv:1405.0301 [hep-ph].

[220] N. D. Christensen and C. Duhr, "FeynRules - Feynman rules made easy," *Comput. Phys. Commun.* **180** (2009) 1614–1641, arXiv:0806.4194 [hep-ph].

[221] A. Alloul, N. D. Christensen, C. Degrande, C. Duhr, and B. Fuks, "FeynRules 2.0 - A complete toolbox for tree-level phenomenology," *Comput. Phys. Commun.* **185** (2014) 2250–2300, arXiv:1310.1921 [hep-ph].

[222] C. Degrande, C. Duhr, B. Fuks, D. Grellscheid, O. Mattelaer, and T. Reiter, "UFO - The Universal FeynRules Output," *Comput. Phys. Commun.* **183** (2012) 1201–1214, arXiv:1108.2040 [hep-ph].

[223] J. Pumplin, D. R. Stump, J. Huston, H. L. Lai, P. M. Nadolsky, and W. K. Tung, "New generation of parton distributions with uncertainties from global QCD analysis," *JHEP* **07** (2002) 012, arXiv:hep-ph/0201195 [hep-ph].

[224] D. S. M. Alves, J. Galloway, J. T. Ruderman, and J. R. Walsh, "Running Electroweak Couplings as a Probe of New Physics," *JHEP* **02** (2015) 007, arXiv:1410.6810 [hep-ph].

[225] D. Becciolini, M. Gillioz, M. Nardecchia, F. Sannino, and M. Spannowsky, "Constraining new colored matter from the ratio of 3 to 2 jets cross sections at the LHC," *Phys. Rev.* **D91** no. 1, (2015) 015010, arXiv:1403.7411 [hep-ph]. [Addendum: Phys. Rev.D92,no.7,079905(2015)].

[226] K. J. Bae, M. Endo, K. Hamaguchi, and T. Moroi, "Diphoton Excess and Running Couplings," arXiv:1602.03653 [hep-ph].

[227] S. Kanemura, Y. Okada, E. Senaha, and C. P. Yuan, "Higgs coupling constants as a probe of new physics," *Phys. Rev.* **D70** (2004) 115002, arXiv:hep-ph/0408364 [hep-ph].

[228] **LHC Higgs Cross Section Working Group** Collaboration, S. Dittmaier *et al.*, "Handbook of LHC Higgs Cross Sections: 1. Inclusive Observables," arXiv:1101.0593 [hep-ph].

[229] S. Dittmaier *et al.*, "Handbook of LHC Higgs Cross Sections: 2. Differential Distributions," arXiv:1201.3084 [hep-ph].

[230] **ATLAS** Collaboration, G. Aad *et al.*, "Measurements of Higgs boson production and couplings in the four-lepton channel in pp collisions at center-of-mass energies of 7 and 8 TeV with the ATLAS detector," *Phys. Rev.* **D91** no. 1, (2015) 012006, arXiv:1408.5191 [hep-ex].

[231] **ATLAS** Collaboration, G. Aad *et al.*, "Measurement of Higgs boson production in the diphoton decay channel in pp collisions at center-of-mass energies of 7 and 8 TeV with the ATLAS detector," *Phys. Rev.* **D90** no. 11, (2014) 112015, arXiv:1408.7084 [hep-ex].

[232] **ATLAS** Collaboration, G. Aad *et al.*, "Search for the $b\bar{b}$ decay of the Standard Model Higgs boson in associated $(W/Z)H$ production with the ATLAS detector," *JHEP* **01** (2015) 069, arXiv:1409.6212 [hep-ex].

[233] "Evidence for Higgs boson Yukawa couplings in the $H \to \tau\tau$ decay mode with the ATLAS detector," Tech. Rep. ATLAS-CONF-2014-061, CERN, Geneva, Oct, 2014.

[234] **ATLAS** Collaboration, G. Aad *et al.*, "Observation and measurement of Higgs boson decays to WW* with the ATLAS detector," *Phys. Rev.* **D92** no. 1, (2015) 012006, arXiv:1412.2641 [hep-ex].

[235] **CMS** Collaboration, V. Khachatryan *et al.*, "Precise determination of the mass of the Higgs boson and tests of compatibility of its couplings with the standard model predictions using proton collisions at 7 and 8 TeV," *Eur. Phys. J.* **C75** no. 5, (2015) 212, arXiv:1412.8662 [hep-ex].

[236] S. Kanemura, Y. Okada, and E. Senaha, "Electroweak baryogenesis and quantum corrections to the triple Higgs boson coupling," *Phys. Lett.* **B606** (2005) 361–366, arXiv:hep-ph/0411354 [hep-ph].

[237] **ATLAS** Collaboration, A. collaboration, "Search for scalar diphoton resonances with 15.4 fb^{-1} of data collected at $\sqrt{s}$=13 TeV in 2015 and 2016 with the ATLAS detector," Tech. Rep. ATLAS-CONF-2016-059, 2016.

[238] **CMS** Collaboration, C. Collaboration, "Search for resonant production of high mass photon pairs using 12.9 fb^{-1} of proton-proton collisions at $\sqrt{s} = 13$ TeV and combined interpretation of searches at 8 and 13 TeV," Tech. Rep. CMS-PAS-EXO-16-027, 2016.

[239] B. Fuks, D. W. Kang, S. C. Park, and M.-S. Seo, "Investigating the jet activity accompanying the production at the LHC of a massive scalar particle decaying into photons," *Phys. Lett.* **B761** (2016) 344–349, arXiv:1608.00084 [hep-ph].